

EPT-M-2011-103

MASTEROPPGAVE

for

Stud.techn. Kyrre Reinertsen
Høsten 2011

Pelton modell turbin test rigg ved Vannkraftlaboratoriet
Pelton model test rig at the Waterpower Laboratory, NTNU

Bakgrunn

Ved Vannkraftlaboratoriet på NTNU er det konstruert og bygget en testrigg for Francis turbiner som tilfredsstiller kravene til IEC 60193. Det er ønskelig å bygge en testrigg for Pelton turbiner som fyller de samme kravene.

Institutt for energi og prosesseteknikk stiller ressurser tilgjengelig til å oppdatere momentmåler og lagerbukk til eksisterende testrigg for Pelton turbiner ved Vannkraftlaboratoriet. Denne oppgaven vil se nærmere på hvordan dette skal gjennomføres og iverksettes.

Mål

Finne optimal løsning for momentmåler og lagerbukk for Pelton turbin testrigg ved Vannkraftlaboratoriet ved NTNU.

Oppgaven bearbeides ut fra følgende punkter

1. Litteratursøk
 - a. Finne relevante publikasjoner der det er beskrevet laboratorieutrustning for modelltest av Pelton turbiner
2. Modell test av Pelton turbin:
 - a. Komplette hill-diagram skal gjennomføres med NTNU's modellturbin
3. Usikkerhetsanalyser:
 - a. Usikkerhetsanalyse skal gjennomføres før og etter oppgradering av testrigg
4. Konstruksjon av lager med måling av lagerfriksjon
 - a. Det skal utarbeides tegninger på lagerbukk med utgangspunkt i tegninger fra Universitetet i Zurich
5. Sammenligning av modelltest før og etter oppgradering av testriggen
6. Dersom det er tid så skal studenten evaluere visualiseringsteknikker for strømming i Pelton skovler.

Senest 14 dager etter utlevering av oppgaven skal kandidaten levere/sende instituttet en detaljert fremdrift- og eventuelt forsøksplan for oppgaven til evaluering og eventuelt diskusjon med faglig ansvarlig/veiledere. Detaljer ved eventuell utførelse av dataprogrammer skal avtales nærmere i samråd med faglig ansvarlig.

Besvarelsen redigeres mest mulig som en forskningsrapport med et sammendrag både på norsk og engelsk, konklusjon, litteraturliste, innholdsfortegnelse etc. Ved utarbeidelsen av teksten skal kandidaten legge vekt på å gjøre teksten oversiktlig og velskrevet. Med henblikk på lesning av besvarelsen er det viktig at de nødvendige henvisninger for korresponderende steder i tekst, tabeller og figurer anføres på begge steder. Ved bedømmelsen legges det stor vekt på at resultatene er grundig bearbeidet, at de oppstilles tabellarisk og/eller grafisk på en oversiktlig måte, og at de er diskutert utførlig.

Alle benyttede kilder, også muntlige opplysninger, skal oppgis på fullstendig måte. For tidsskrifter og bøker oppgis forfatter, tittel, årgang, sidetall og eventuelt figurnummer.

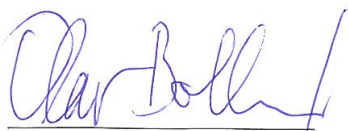
Det forutsettes at kandidaten tar initiativ til og holder nødvendig kontakt med faglærer og veileder(e). Kandidaten skal rette seg etter de reglementer og retningslinjer som gjelder ved alle (andre) fagmiljøer som kandidaten har kontakt med gjennom sin utførelse av oppgaven, samt etter eventuelle pålegg fra Institutt for energi- og prosesssteknikk.

Risikovurdering av kandidatens arbeid skal gjennomføres i henhold til instituttets prosedyrer. Risikovurderingen skal dokumenteres og inngå som del av besvarelsen. Hendelser relatert til kandidatens arbeid med uheldig innvirkning på helse, miljø eller sikkerhet, skal dokumenteres og inngå som en del av besvarelsen.

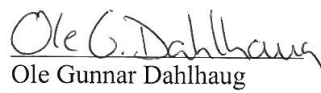
I henhold til ”Utfyllende regler til studieforskriften for teknologistudiet/sivilingeniørstudiet” ved NTNU § 20, forbeholder instituttet seg retten til å benytte alle resultater og data til undervisnings- og forskningsformål, samt til fremtidige publikasjoner.

Besvarelsen leveres digitalt i DAIM. Et faglig sammendrag med oppgavens tittel, kandidatens navn, veileders navn, årstall, instituttnavn, og NTNUs logo og navn, leveres til instituttet som en separat pdf-fil. Etter avtale leveres besvarelse og evt. annet materiale til veileder i digitalt format.

NTNU, Institutt for energi- og prosesssteknikk, 22. august 2011



Olav Bolland
Instituttleder



Ole Gunnar Dahlhaug
Faglig ansvarlig/veileder

Medveileder(e) Torbjørn K. Nielsen
 Bjørn Winther Solemslie, PhD-student

Preface

This master thesis was written by Kyrre Reinertsen at the Water Power Laboratory at the Norwegian University of Science and Technology during the fall of 2011. The goal of this thesis was to upgrade the pelton turbine test rig to meet international standards.

They say all is well that ends well, and thanks to all the help I have had during this semester, this thesis has been a great experience and a great ending of my studies.

I would like to thank my supervisor and co-supervisor Ole Gunnar Dahlhaug and Bjørn Winther Solemslie for good guidance during the course of this project. Many thanks goes to Thomas Staubli at Hochschule Luzern for sharing with us their bearing design and for all help during the design process.

Most of all I must thank Bård Brandåstrø for trusting me with this project, for always being helpful and for pushing the project forward, and without the effort of Joar Grilstad, Trygve Opland and Halvor Haukvik, the new test rig would not have been ready in time for testing.

Finally I want to give credit to all the students and employees at the Water Power laboratory for creating such a great and motivational atmosphere which have made the last year at NTNU very special.

Kyrre Reinertsen
Trondheim, January 23, 2012

Sammendrag

Vannkraftlaboratoriet ønsker å bygge en testrigg for peltonturbiner som tilfredstiller kravene til IEC 60193. Den eksisterende riggen må oppgraderes og det må implementeres mulighet for måling av friksjonsmomentet. I denne oppgaven vil det designes, maskineres og installeres ny lagerbukk med mulighet for friksjonmåling. IEC 60193 gjennomgås med hovedvekt på laboratorieutrustning og måleusikkerhet for å se hvilke krav som må tilfredstilles. Et komplett hilddiagram kjøres før og etter oppgraderingen og det gjøres usikkerhetsanalyser på resultatene. Videre sammenlignes og analyseres virkningsgradkurvene med og uten friksjonsmoment.

Oppgraderingen av Testriggen viser seg å være en suksess. Den gir gode stabile målinger og tilfredstiller IECs krav til usikkerhet. Den står nå klar til å gi nøyaktige målingeresultater for videre forskning på peltonturbiner.

Abstract

The Water Power Laboratory at NTNU wished to construct a test rig for pelton turbines that complied with IEC 60193. The existing test rig lacked the ability to measure friction torque and this master thesis was aimed to find an optimal solution for an upgrade that made this possible. The IEC 60193 is studied to see which requirements need to be fulfilled, both for instrumentation and measurement uncertainty in order to be compliant with the standard.

A new bearing block, featuring friction torque measurements, is designed, machined and installed in the old test rig. Model tests are performed before and after upgrading to produce complete hill diagrams and efficiency curves for comparison. Uncertainty analyses are done on both tests and compared with the limits set by the IEC standard.

The upgrade of the test rig proved to be a success. It gives reliable measurements with a good repeatability and it is found to fulfill the requirements set by IEC for a model test rig. The Water Power laboratory now has the test rig required to continue research and developement of the pelton turbine.

Contents

1	Introduction	1
2	Testing of Pelton Turbines	3
2.1	Objective	3
2.2	Instruments and Measurements	4
2.2.1	Discharge	4
2.2.2	Pressure	4
2.2.3	Torque	5
2.2.4	Rotational speed	5
2.2.5	Uncertainties in measurements	5
2.2.6	Final test report	6
2.3	Previous Work	7
2.3.1	Efficiency	7
2.3.2	Uncertainty	8
2.3.3	Friction Test	8
3	Pelton Turbine Efficiency	9
3.1	Efficiencies	9
3.1.1	Hydraulic Efficiency	9
3.1.2	Mechanical Efficiency	9
3.1.3	Efficiency	10
3.2	Power	10
3.2.1	Mechanical Power	10
3.2.2	Hydraulic Power	10
3.3	Reduced Values	11
4	Experimental Setup	13
4.1	Object	13
4.2	Test Rig	13
4.3	Test Model Runner	14

4.4	Instrumentation	14
4.4.1	Torque and Rotational Speed	14
4.4.2	Friction Torque	15
4.4.3	Volume Flow	15
4.4.4	Hydraulic Energy	16
4.5	Test Procedure	16
4.5.1	Hill Diagram	16
4.5.2	Friction Test	16
4.6	Postprocessing	17
5	Uncertainty analysis	19
5.1	Types of errors	19
5.1.1	Random errors	20
5.1.2	Systematic errors	20
5.2	Uncertainty in Calibration	21
5.2.1	Regression Error	21
5.3	Total uncertainty	22
5.4	Uncertainty in Pelton Model Tests	22
5.4.1	Discharge Q	23
5.4.2	Torque	23
5.4.3	Rotational speed	24
5.4.4	Water Density	24
5.4.5	Hydraulic energy E	24
6	Bearing Design	27
6.1	Bearing Concept	28
6.2	Bearing modifications	28
6.2.1	Maximum deflection	29
6.2.2	Resonance	30
6.3	Water Control	31
6.4	Installation	32
6.5	Production	32
7	Results	33
7.1	Efficiency	34
7.1.1	Comparing the hydraulic and total efficiency	36
7.2	Friction Torque Verification	38
7.3	Uncertainties and Repeatability	40
7.3.1	Uncertainties	40
7.3.2	Repeatability	41
7.4	New Test Rig	42

8	Discussion	45
8.1	Efficiency	45
8.2	Friction Torque Measurements	46
8.3	Repeatability	46
8.4	Uncertainties	47
9	Conclusion	49
A	Calibration of Friction Torque	I
A.1	The system	I
A.1.1	Description	I
A.1.2	Equipment used in Calibration	II
A.2	Calibration	III
A.2.1	Preparation	III
A.2.2	Calibration	III
A.2.3	Note	IV
B	Systematic Uncertainty Before Upgrade	V
B.1	Hydraulic energy E	V
B.2	Discharge Q	VI
B.3	Torque	VII
B.4	Summary of Uncertainties	VIII
C	Systematic Uncertainty After Upgrade	IX
C.1	Torque	IX
C.1.1	Shaft torque	IX
C.1.2	Friction Torque	X
C.1.3	Mechanical Torque	XI
D	Calibration Data Before Upgrading	XIII
E	Calibration Data After upgrade	XIX
F	Parts and Materials	XXVII
G	Machine Drawings	XXXI
G.1	Matlab Source Code	LII
G.1.1	Import Raw Data	LII
G.1.2	Calculate Mean Data	LIII
G.1.3	Efficiency Curve Fit	LVIII
G.1.4	Plot Hill Chart	LXI
G.1.5	Uncertainty due to the Regression Process	LXII

List of Figures

2.1	Hill diagram for the reference runner at a static pressure of 760 kPa. [1]	7
4.1	Pelton Turbine Test Rig [1]	14
4.2	The reference model	15
4.3	Measuring points recorded for the efficiency tests.	17
6.1	Old bearing block assembly.	27
6.2	CAD drawing of the existing design.	28
6.3	Section view of the existing design.	28
6.4	Method of calibrating and measuring the friction	29
6.5	Section view of the bearings.	29
6.6	Model of the forces applied to the Turbine shaft	29
6.7	Shaft Properties	30
6.8	Three circular disks directing water away from the shaft.	31
6.9	Three quarter section view of the cover.	31
6.10	Bearing block placed on two beams	32
7.1	Hill diagram before and after the upgrade.	35
7.2	The graph shows the efficiency before and after upgrading, with and without the friction torque for constant volume flow.	37
7.3	Efficiency curve with total uncertainties at best nozzle opening before and after upgrade.	37
7.4	Friction torque tests performed without water.	39
7.5	The graph shows the hydraulic and total efficiency recorded for 14mm nozzle opening on two different days.	41
7.6	The graph shows the variation in measured efficiency at the same operation point on five days	42
7.7	Pictures of the upgraded test rig.	43
A.1	Friction torque Calibration Setup	II

List of Tables

2.1	Systematic uncertainties that should be obtained according to IEC 60193.	6
2.2	Results by Trefall	8
7.1	Uncertainties before upgrade	40
7.2	Uncertainties after upgrade	40
A.1	Calibration Points	III
B.1	Uncertainties before upgrade	VIII
C.1	Uncertainties after upgrade	XI

Nomenclature

Symbols

Symbol		Unit
A	Cross sectional area of inlet pipe	m^2
D	Diameter Runner	m
E	Specific Hydraulic Energy	W
e_X	Absolute uncertainty in the measurement X	—
F	Force	N
f_X	Relative uncertainty in the measurement X	%
g	Gravity	m/s^2
H_e	Effective Head	m
m	Mass	kg
N	Number of measurements	—
n	Rotational speed	rpm
n_{11}	Modified speed factor	—
n_{ED}	Speed factor	—
p_1	Inlet Pressure	Pa
P	Power	W
P_h	Hydraulic Power	W
P_m	Mechanical Power	W
P_{Lm}	Power loss due to friction in bearings	W
p	Pressure	Pa
Q	Volumetric flow	m^3/s
Q_{ED}	Discharge factor	—
T	Torque	Nm
v_1	Inlet Velocity of the water where the inlet pressure is measured	m/s
Z	Number of Buckets	—

Greek Letters

Symbol	Meaning	Unit
η_h	Hydraulic Efficiency	—
η_m	Mechanical Efficiency	—
η	Efficiency	—
π	Constant	—
ρ	Water Density	kg/m^3
ω	Angular Velocity	rad/s

Sub symbols

<i>abs</i>	Absolute
<i>gen</i>	Generator
<i>Lm</i>	Friction
<i>tot</i>	Total
<i>r</i>	Random
<i>s</i>	Systematic
<i>ED</i>	Reduced Variable
11	Modified Variable

Abbreviations

BEP	Best Efficiency Point
RMS	Root-Mean-Square Method
RSS	Root-Sum-Square Method
NTNU	Norwegian University of Science and Technology

Chapter 1

Introduction

As the battle for higher efficiency has come to be about a tenth of a percent, the accuracy of the turbine test rigs becomes ever more important. The Water Power Laboratory in Trondheim has long made due without measuring the friction torque when testing Pelton turbines. To comply with the international standards it is necessary to be able to measure this friction. The existing test rig was based on the swinging frame method for measuring the friction torque, though the swinging frame was bolted and welded together years ago. To measure the friction, the test rig needs to undergo an upgrade.

Chapter 2

Testing of Pelton Turbines

No international standard as such exists for the procedures for hydraulic model turbine tests. There is however an international consensus of opinion on the matter. The International Electrotechnical Commission is a worldwide organization for the standardization comprising all national electrotechnical committees. The object of the IEC is to promote international co-operation on all questions concerning standardization in the electrical and electronic fields. IEC [2] is a document giving recommendation for international use and is published in the form of standards, technical reports or guides and they are accepted by the National Committees in that sense.

2.1 Objective

The objective of the standard is:

- to define the terms and quantities used;
- to specify methods of testing and of measuring the quantities involved, in order to ascertain the hydraulic performance of the model;
- to specify methods of computation of results and of comparison with guarantees;
- to determine if the contract guarantees which fall within the scope of this standard, have been fulfilled;
- to define the extent, content and structure of the final report.

For our purposes IEC [2] will specify methods of testing and of measuring the involved quantities and to define the extent and content of the final report.

2.2 Instruments and Measurements

A thorough description of most instruments and quantities used for measuring is given in the IEC. Those relevant for our model test will be described in the following section.

2.2.1 Discharge

The IEC Standard identifies primary and secondary methods for measuring discharge. Primary methods are those involving only fundamental quantities. For our model test the secondary method is used measuring the discharge with an electromagnetic flow meter. Electromagnetic flow meters have the advantage that they do not generate disturbances in the flow or pressure losses. They are also not very sensitive to wear. They produce instantaneous readings and are particularly convenient for detecting discharge fluctuations.

Any device used for discharge measurements shall be calibrated against a primary method. Calibration shall be made without dismantling the flow meter from the test circuit or modifying the flow conditions at the inlet of the flow meter. It should be carried out in the actual operating conditions prevailing during the tests and shall include sufficient measuring points evenly distributed over the whole range of the discharge to be measured during tests. The secondary flow meter should normally be calibrated before and after the tests.

If the installation is carefully constructed, maintained and the above requirements are satisfied, a systematic uncertainty on the discharge measurements within $\pm 0.2\%$ to $\pm 0.3\%$ can be achieved.

2.2.2 Pressure

For a Pelton turbine the pressure measurements are used to determine the specific hydraulic energy. As for discharge measurements the pressure measurements can be made using primary and secondary methods. Dead weight

manometer is a primary method while a secondary method using a pressure transducer is used in our tests. The pressure transducer must be calibrated using a primary method. It shall be calibrated under the test pressure conditions. IEC [2] estimates that a systematic uncertainty of $\pm 0.1\%$ to $\pm 0.5\%$ should be expected if using a pressure transducer.

2.2.3 Torque

Torque is measured to determine the mechanical power of the runner. The true mechanical torque applied to the runner is T_m and is equal to the shaft torque T plus the friction torque T_{Lm} .

Two different measurement systems are described in the IEC standard. The swinging frame type measures the mechanical torque T_m while the second method measures the friction torque separately. The swinging frame method was used in our laboratory previously but was replaced by the second method using a torque transducer. IEC describes many ways of measuring torque. The swinging frame method is favorized for torque measurements. Torque meters may be used provided its accuracy is acceptable and it is calibrated using the primary method. The systematic uncertainty in the shaft torque should be within 0.15-0.25 %. The systematic uncertainty achieved for the friction torque should be within 0.02-0.05 %.

2.2.4 Rotational speed

IEC mentions different ways of measuring the rotational speed. They have in common that rather than being calibrated they are checked. Ways for checking the rotational speed can be another speed measurement device or by checking separately the counting of pulses and the accuracy of the time base. The systematic uncertainty is expected to be within 0.01-0.05 %

2.2.5 Uncertainties in measurements

Table 2.1 summarizes the systematic uncertainties IEC [2] states one should be able to achieve:

Measurement	Systematic Uncertainty
Hydraulic energy	$\pm 0.1 - 0.5\%$
Discharge	$\pm 0.1 - 0.2\%$
Torque	$\pm 0.15 - 0.25\%$
Friction Torque	$\pm 0.02 - 0.05\%^*$
Rotational Speed	$0.01 - 0.05\%$

Table 2.1: Systematic uncertainties that should be obtained according to IEC 60193.

2.2.6 Final test report

¹ The final test report should include:

- Object and purpose of the test;
- Personnel taking part in the tests;
- Description of the model together with drawings showing the main section of the model and its general arrangement in the test rig;
- Description of the test rig and the measuring equipment, including calibration methods and data processing;
- Calibration data and inspection reports;
- Test procedures for the tests;
- Calculation of uncertainties of measurement with reference to the calibration data;
- Discussion and interpretation of test results.

¹*% of total torque.

2.3 Previous Work

Being the main test rig for pelton turbines, there have been done many efficiency tests throughout the years. The latest work was done by Stine Trefall in the spring of 2011 [1]. An efficiency test was done on three pelton runners including the reference runner owned by the laboratory.

2.3.1 Efficiency

Trefall tested the reference model with a static pressure of 760 kPa and 260 kPa. Her results are presented in table 2.2

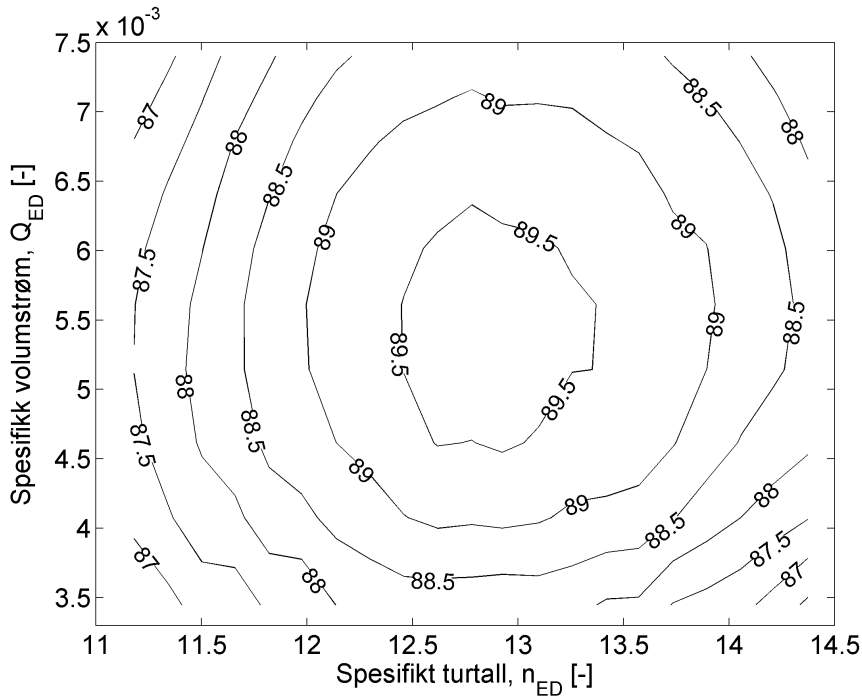


Figure 2.1: Hill diagram for the reference runner at a static pressure of 760 kPa. [1]

Test	$p_{stat}[kPa]$	Best efficiency [%]	$n_{ED}[-]$	$Q_{ED}[-]$
Trefall # 1	760	$89,70 \pm 0,41$	12,8	0,0056
Trefall # 2	260	$88,08 \pm 0,82$	12,5	0,0068

Table 2.2: Results by Trefall

2.3.2 Uncertainty

Trefall identifies that the uncertainty in the discharge measurements had the greatest impact in the uncertainty for the high pressure test while the uncertainty related torque and pressure dominated in the low pressure test.

2.3.3 Friction Test

Trefall did friction tests with the test rig. Which runner that was tested is unclear but a comparison will be made after the upgrade is complete.

Chapter 3

Pelton Turbine Efficiency

3.1 Efficiencies

Three types of efficiencies are considered in this paper;

1. Hydraulic Efficiency
2. Mechanical Efficiency
3. Efficiency, or Total Efficiency

3.1.1 Hydraulic Efficiency

The hydraulic efficiency η_h of a Pelton turbine is defined as:

$$\eta_h = \frac{P_m}{P_h} \quad (3.1.1.1)$$

Where P_m is the power delivered to the turbine shaft by the runner, and P_h is the available hydraulic power in front of the nozzle.

$$P_h = E(\rho Q) \quad (3.1.1.2)$$

3.1.2 Mechanical Efficiency

The mechanical efficiency η_m is defined as:

$$\eta_h = \frac{P_{gen}}{P_m} \quad (3.1.2.1)$$

where P_{gen} is the power delivered to the generator after the friction power is subtracted.

3.1.3 Efficiency

What IEC [2] defines as efficiency is the total efficiency of the hydraulic machine;

$$\eta = \frac{P_{gen}}{P_h} \quad (3.1.3.1)$$

$$\eta = \eta_h \cdot \eta_m \quad (3.1.3.2)$$

3.2 Power

3.2.1 Mechanical Power

The mechanical power is the power delivered from the turbine runner to the turbine shaft. This consist of the power delivered to the generator P_{gen} plus the power lost in the bearings P_{Lm} due to friction.

$$P_m = P_{gen} + P_{Lm} \quad (3.2.1.1)$$

The power is a function of Torque and rotational speed.

$$P_m = T_m \cdot \omega = T_m \cdot \frac{\pi \cdot n}{30} \quad (3.2.1.2)$$

3.2.2 Hydraulic Power

The hydraulic power, P_h is defined as the available power in front of the nozzle. This includes the static and dynamic pressure.

$$P_h = E\rho Q \quad (3.2.2.1)$$

$$E = \frac{p_{abs1} - p_{abs2}}{\rho} + \frac{v_1^2 - v_2^2}{2} + (z_1 - z_2)g \quad (3.2.2.2)$$

In the test rig the pressure measured in front of the nozzle, p_1 , is the relative static pressure. The outlet pressure, p_2 is regarded as atmospheric pressure and can be disregarded. The inlet velocity, v_1 depends on the discharge while the velocity after the runner, v_2 regarded as lost and set to zero. z_1 is the difference in height between the center of the nozzle and where the pressure is measured.

$$E = \frac{p_1}{\rho} + \frac{v_1^2}{2} + (z_1)g \quad (3.2.2.3)$$

The density will vary slightly with temperature and pressure and is calculated from the temperature and pressure measurements using equation found in IEC [2] section 2.5.3.1.3.

3.3 Reduced Values

Using reduced values in model testing helps comparing the results to models of different sizes and makes scaling the results easier. In our test we will use the dimensionless parameters Q_{ED} and n_{ED} as well as the modified parameters Q_{11} and n_{11} . All results will be presented using these reduced parameters. For our purposes this helps us compare the results with results done with different heads.

$$n_{ED} = \frac{n \cdot D}{\sqrt{g \cdot H_e}}, \quad Q_{ED} = \frac{Q}{D^2 \sqrt{g \cdot H_e}}, \quad (3.3.0.4)$$

$$n_{11} = \frac{n \cdot D}{\sqrt{H_e}}, \quad Q_{11} = \frac{Q}{D^2 \sqrt{H_e}}, \quad (3.3.0.5)$$

Chapter 4

Experimental Setup

4.1 Object

The objectives of the experiment are to:

- Perform an efficiency test on the reference runner;
- Produce a complete hill diagram;
- Quantify the friction losses in the bearings;
- Test for repeatability in the measurements;
- Quantify the uncertainty in the results;

4.2 Test Rig

The tests are run at the Water Power Laboratory at NTNU using the laboratory's reference turbine in the Pelton Turbine Test Rig. Figure 4.1 shows the setup of the Test Rig in the laboratory. The pump supplies the turbine with the desired pressure and discharge. The valve to the right in figure 4.1 is used to direct water to the weighing tank used for calibration of the volume flow meter.

The pump has a capacity of 100 l/s at 100 m effective head. The test rig is fully automated. The pump's rotational speed, the discharge and the runner's rotational speed is set from the control room.

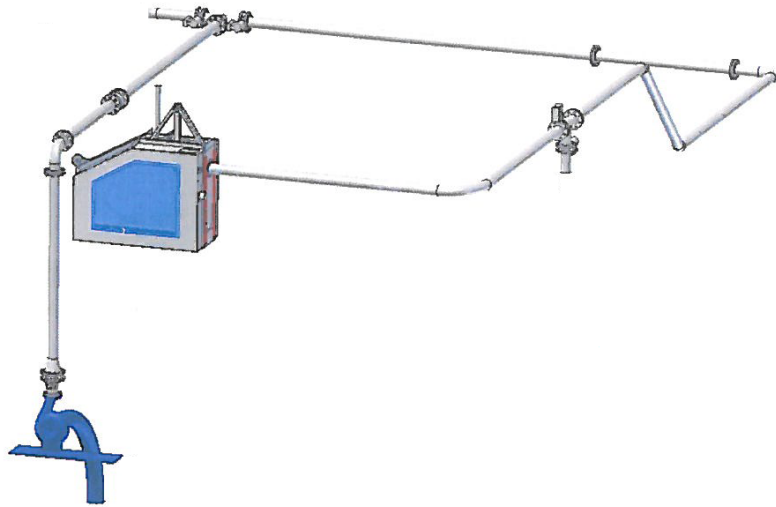


Figure 4.1: Pelton Turbine Test Rig [1]

4.3 Test Model Runner

The tests are done on the Water Power Laboratory's reference model. The model is a Pelton runner produced by Kværner that has been chosen to serve as a reference to future tests and a way of checking that the test rig gives consistent readings. The reference model has a diameter of 0.479m and has 22 buckets. Figure 4.2 shows the reference model.

4.4 Instrumentation

All measurement devices are calibrated before each test and the calibration reports can be found in Appendix D. They are all connected to an amplifier in the control room that prepares the signals to be logged using Labview.

4.4.1 Torque and Rotational Speed

Both of the torque transducers are made by Hottinger Baldwin Messtechnik and have a range of 0-500 Nm. In the first setup we use a HBM T22, while in the second setup we will install a HBM T10F/FS.

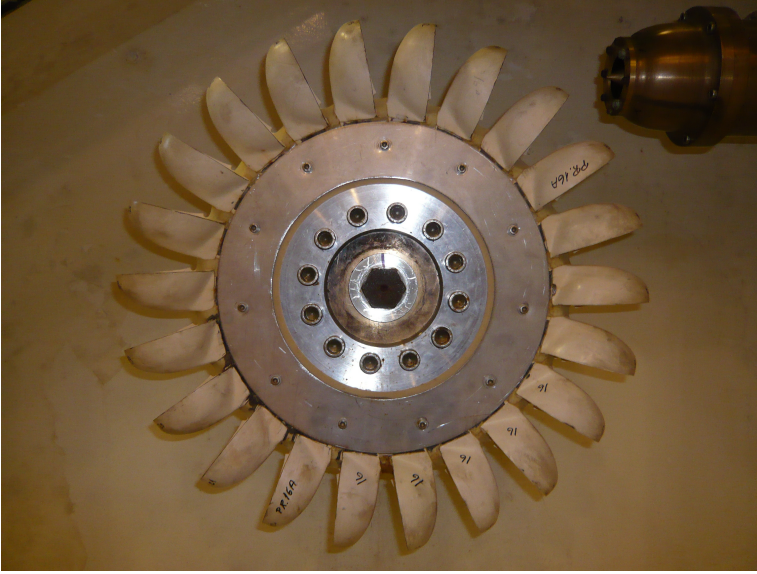


Figure 4.2: The reference model

The torque transducers are calibrated using the primary method with calibrated weights. They are calibrated in the range 0-500 Nm. The calibration data is presented in Appendix D

4.4.2 Friction Torque

The friction torque is measured with a Z6 beam force cell produced by HBM. The force cell has a nominal load of 5 kg, which with a lever arm of 0.25m, gives it a measurement range of 0-12.5 Nm. Since the friction torque is a new feature on the pelton turbine test rig, a new procedure for calibration had to be developed. A few problems were encountered when starting to calibrate and a few necessary actions had to be taken to get a good reading and calibration. A procedure is made and put in Appendix A.

4.4.3 Volume Flow

The volume flow is measured with an electromagnetic flow sensor. The Instrument used is an Optiflux F made by Krohne.

The volume flow meter is calibrated using a secondary method by weighing.

A constant flow rate is run through the flow meter into the weighing tank for a measured period of time, while recording the output signal from the flow meter. This is done for 12 different flow rates in the range 0-65 l/s to obtain a calibration curve. The calibration data is presented in D.

4.4.4 Hydraulic Energy

The hydraulic energy depends on pressure and the density of water, which in turn depends on the temperature.

The pressure is measured with a pressure transducer produced by Tecsis. The pressure transducer is calibrated with the secondary method using a calibrated dead weight manometer. It is calibrated in the range 0-100 m.

4.5 Test Procedure

4.5.1 Hill Diagram

The test run and calibration before upgrading was done in cooperation with Lorentz Fjellanger Barstad. The conditions were kept constant before and after upgrading. The effective head was kept at 70 m throughout the test. To obtain the hill diagram the nozzle opening and rotational speed of the runner was varied. The points of operation to record were chosen based on previous work done by Trefall [1] to get the BEP in the center of the hill diagram. Figure 4.3 shows the operation points that were recorded to produce the hill diagrams. Every point was recorded in steady conditions for 40 seconds.

4.5.2 Friction Test

To check the friction torque measurements against the shaft torque, a friction test was performed.

The turbine was set at a constant rotational speed using the generator as a motor. Then the friction in both the shaft and bearings were recorded for 30 seconds. This was done for rotational speeds up to 1000 RPM

The same test was then done without the turbine runner attached. The results can be found in section 7.2.

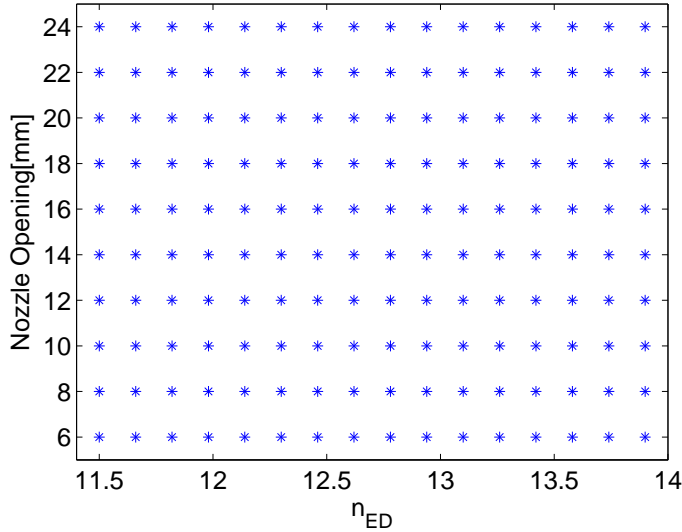


Figure 4.3: Measuring points recorded for the efficiency tests.

4.6 Postprocessing

All measurements are recorded from the control room. The volt or frequency signals from all devices are processed in Labview during tests. Labview gives out two output files. One contains the raw data of the measurements and another contains the processed mean data. The raw data was then processed with the Matlab scripts, *import_data.m* and *meandata_create.m*, made by Lorentz Fjellanger Barstad to obtain the mean data, a hill diagram, and compute the random uncertainties. The scripts used can be found in Appendix G.1.1. The raw and mean data are appended digitally as the matlabfiles: *rawdata1.mat*, *rawdata2.mat*, *meandata1.mat* and *meandata2.mat*.

Chapter 5

Uncertainty analysis

An uncertainty analysis is done on the measurements before and after upgrading. An Error analysis is the study and evaluation of uncertainty in the measurements. All measurements, however carefully made, are subject to errors. Error in a scientific measurement means the inevitable uncertainty that attends all measurements. IEC [2] defines errors as the difference between a measurement and the true value of the quantity. The range within which the true value of a measured quantity can be expected to lie, with a suitably high probability, is termed the uncertainty in the measurement. IEC [2] uses a 95 % confidence level. This is saying that the true value of a measured quantity has a probability of 95% to lie within the given range.

5.1 Types of errors

IEC [2] considers three types of error:

- Spurious errors
- Random errors
- Systematic errors

Spurious errors are errors caused by human errors or malfunctioning instruments. These errors invalidate the measurements and they must be discarded. Examples of spurious errors can be pockets of air in the tube going to the pressure manometer or numbers being transposed while recording the data.

5.1.1 Random errors

Random errors are caused by numerous, small, independent influences which prevent a measurement system from delivering the same reading when supplied with the same input value. The measurements deviate from the mean in accordance with the laws of chance, such that their distribution usually approaches a normal (Gaussian) distribution as the number of measurements is increased.

Random errors can be decreased by doing the experiments thoroughly and by increasing the number of measurements. The repetition of points at given operation condition enables us to use statistical methods to determine the uncertainty associated with random errors. When the sample size is small, it is necessary to correct the statistical results that are based on the assumption of a normal distribution. Student-t distribution compensates for the fact that uncertainty in the standard deviation is increasing with decreasing sample size. Although the number of measurements can always be increased to obtain a lower uncertainty, the IEC [2] advise that when the random uncertainty is less than the maximum limit of 0.1% it is set to this value.

5.1.2 Systematic errors

Systematic errors are usually categorized as instrumental, personal or external. An instrumental error is due to faults or limitation of the measuring device. This includes improper calibration and broken devices. Personal errors vary from one observer to the next and indicate any bias the observer may have. External errors are introduced by the environment in which the measurements are taken [3]. Systematic errors are present prior to doing the measurements and cannot be reduced by increasing the number of measurements. To estimate the uncertainty associated with systematic errors one must identify each component which can influence its value. Examples of systematic errors can be a stopwatch running consistently slower, or a ruler being slightly longer than what it should be. The total systematic error is mainly given by the systematic error due to the calibration of the secondary instrument, and by the errors in physical properties. In most cases the systematic error may be taken as equal to the total uncertainty in calibration of the secondary instrument used for measuring the quantity. $f_d \cong f_{tcal}$ [2]

5.2 Uncertainty in Calibration

IEC [2] lists six sources of errors that can arise during calibration: Although some of them being random in nature, they become systematic errors when running the measurements.

- (a) Bias of the primary method: this is the systematic component of the intrinsic error of the primary method used for the calibration: $\pm f_a$.
- (b) Repeatability of the primary method: this is the random component of the intrinsic error of the primary method used for the calibration: $\pm f_b$.
- (c) Bias of the secondary instrument: this is the systematic component of the intrinsic error of the secondary instrument: $\pm f_c$.
- (d) Repeatability of the secondary instrument: this is the random component of the intrinsic error of the secondary instrument: $\pm f_d$.
- (e) Errors due to physical phenomena and influence quantities: $\pm f_e$.
- (f) Errors in physical properties: these are the errors arising in the determination of physical quantities either by direct measurement or from international standardized data: $\pm f_f$.

All the errors listed above can be combined using the root-sum-square method. This results in the relative uncertainty in the calibration curve:

5.2.1 Regression Error

The regression line for the calibrations is fitted using the method of least squares. The error and uncertainty that is introduced is due to the fact that the data points will not be exactly on the regression line. The procedure for finding the uncertainty is described in Warpole [4]

To find the uncertainty along the calibration curve the uncertainty in each point 5.2.1.1 must be calculated for every y-value and its corresponding x-value. These points can then be used to establish the uncertainty band for the regression line:

$$f_{Y|x_0} = \pm t_{\alpha/2} \cdot \sqrt{\frac{1}{n} + \frac{(x_0 - \bar{X})^2}{S_{xx}}} \quad (5.2.1.1)$$

where

$$S_{xx} = \sum_{i=1}^n (x_i - \bar{x})^2 \quad (5.2.1.2)$$

$$S_{yy} = \sum_{i=1}^n (y_i - \bar{y})^2 \quad (5.2.1.3)$$

$$S_{xy} = \sum_{i=1}^n (x_i - \bar{x})(y_i - \bar{y}) \quad (5.2.1.4)$$

$$s^2 = \frac{S_{yy} - bS_{xy}}{n - 2} \quad (5.2.1.5)$$

$$b = \frac{S_{xy}}{S_{xx}} \quad (5.2.1.6)$$

5.3 Total uncertainty

When the random and systematic uncertainties are found, they are combined using the RSS-method into the total uncertainty. For the hydraulic efficiency the total uncertainty is given by equation 5.3.0.7:

$$f_{\eta_t} = \pm \sqrt{f_{\eta_s}^2 + f_{\eta_r}^2} \quad (5.3.0.7)$$

5.4 Uncertainty in Pelton Model Tests

In this section, the uncertainties involved in pelton model turbine tests are investigated and presented. The calculation of the uncertainties can be found in Appendix B.

The total systematic and random uncertainty for hydraulic efficiency consists of the individual uncertainties in discharge, specific hydraulic energy, torque, speed of rotation and density of water:

$$(f_{\eta})_s = \pm \sqrt{(f_Q)_s^2 + (f_E)_s^2 + (f_T)_s^2 + (f_n)_s^2 + (f_{\rho})_s^2} \quad (5.4.0.8)$$

$$(f_{\eta})_r = \pm \sqrt{(f_Q)_r^2 + (f_E)_r^2 + (f_T)_r^2 + (f_n)_r^2 + (f_{\rho})_r^2} \quad (5.4.0.9)$$

Finding and computing all the individual uncertainties is necessary to determine the total uncertainty in the hydraulic efficiency.

5.4.1 Discharge Q

The discharge is measured by an electromagnetic flow meter which is a secondary instrument. The flow meter is calibrated with the primary method of weighing. The weighing is done by a weighing tank which itself must be calibrated. A thorough analysis of the uncertainties related to the calibration by weighing has been done by Storli [5]. Storli [5] used the same flow meter and his findings are found to be valid also in our model test:

$$f_{Q_{cal}} = \pm \sqrt{(f_{\Delta m})^2 + (f_{div})^2 + (f_{\rho_m})^2 + (f_{\Delta m})_t^2 + (f_{div})_s^2 + (f_{Q,reg})^2} \quad (5.4.1.1)$$

$f_{\Delta m}$	The systematic uncertainty related to the calibration of the weighing machine.
f_{div}	The systematic uncertainty related to the operation of the diverter
f_{ρ_m}	Uncertainty related to the determination of the density
$f_{\Delta m_r}$	The random uncertainty related to the calibration of the weighing machine.
f_{div_s}	The random uncertainty related to the operation of the diverter
$f_{Q,reg}$	The uncertainty that arises from the regression process used to determine the calibration curve.

5.4.2 Torque

The systematic uncertainty of the torque measurements are related to the calibration of the torque transducers. The first setup only measures the shaft torque T while after the upgrade we will have an uncertainty for both the shaft torque T and the friction torque T_{Lm}

For the first setup we have the systematic uncertainty due to calibration:

$$f_{T_{cal}} = \pm \sqrt{(f_{TW})^2 + (f_{T_{arm}})^2 + (f_{T_{reg}})^2} \quad (5.4.2.1)$$

where

- f_{T_W} The systematic uncertainty related to the weights used for calibration.
- $f_{T_{arm}}$ The systematic uncertainty related to the measuring of the length of the lever arm.
- $f_{T_{reg}}$ The uncertainty that arises from the regression process used to determine the calibration curve.

For the second setup where we measure the friction torque we will have a slightly different uncertainty:

$$f_{T_{cal}} = \pm \frac{\sqrt{(e_{T_{gen}})^2 + (e_{T_{Lm}})^2}}{T_{tot}} \quad (5.4.2.2)$$

Where the individual errors will be calculated as for the first setup.

$$e_{T_{Lm}} = \pm T_{Lm} \cdot \sqrt{(f_{T_W})^2 + (f_{T_{arm}})^2 + (f_{T_{reg}})^2} \quad (5.4.2.3)$$

5.4.3 Rotational speed

The rotational speed is generally not calibrated, rather checked by comparison with another speed measuring device. IEC [2] states that the systematic uncertainty f_{n_s} is expected to be within the range of 0,01 % to 0,05%. $f_{n_s} = 0,025$ is used for our model test.

5.4.4 Water Density

Water density is a function of pressure and temperature. Change in any of these has very little effect on the density of water. As the uncertainties related to these properties are very low, the total influence on the uncertainty in hydraulic efficiency by the uncertainty in water density is neglected.

5.4.5 Hydraulic energy E

The hydraulic energy for a Pelton turbine depends on the pressure and inlet velocity at the location of the pressure transducer. It is assumed that the uncertainty in gravity and water density is negligible for the uncertainty in hydraulic energy.

$$f_E = \pm \frac{e_E}{E} = \pm \frac{\sqrt{(\frac{e_p}{\rho})^2 + (g \cdot e_{z_{dif}})^2 + (\frac{e_{v_1^2}}{2})^2}}{\frac{p}{\rho} + g e_{z_{dif}} + \frac{e_{v_1^2}}{2}} \quad (5.4.5.1)$$

E	Total hydraulic energy.
e_E	Absolute error in hydraulic energy
e_p	Absolute error in inlet pressure
$e_{z_{dif}}$	Absolute error in the measured difference in height between the pressure transducer and the inlet
$\frac{e_{v_1^2}}{2}$	Absolute error in inlet velocity

where

$$\frac{e_p}{\rho} = \frac{p}{\rho} \cdot f_{p_s} \quad (5.4.5.2)$$

$$\frac{e_{v_1^2}}{2} = v_1^2 \cdot f_{v_1} \quad (5.4.5.3)$$

the relative systematic uncertainty f_{p_s} is the uncertainty related to the regression process determining the calibration curve for the pressure transducer. The uncertainty f_{v_1} is the uncertainty in the cross sectional area of the inlet tube and the calculated inlet velocity determined by the discharge Q .

$$f_{p_s} = \pm \sqrt{(f_{p_{ab}})^2 + (f_{p_{reg}})^2} \quad (5.4.5.4)$$

$$f_{v_{1s}} = \pm \sqrt{(f_{A_i})^2 + (f_{Q_t})^2} \quad (5.4.5.5)$$

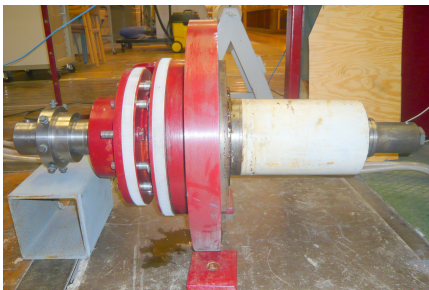
$f_{p_{ab}}$	Uncertainty in the dead weight manometer used for calibrating the pressure transducer.
$f_{p_{reg}}$	Uncertainty in the regression process used in establishing a calibration curve.
f_{Q_t}	Total uncertainty in the discharge measurement.
f_{A_i}	Uncertainty in the inner cross-sectional area of the inlet tube.

Chapter 6

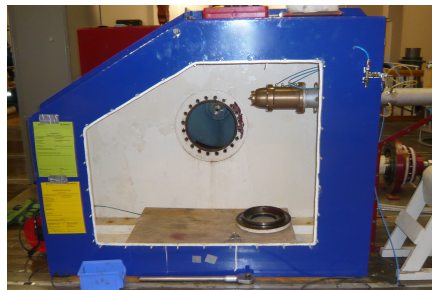
Bearing Design

Figure 6.1(a) 6.1(b) shows the old bearing block and where it was mounted in the turbine housing.

The new bearing block must fit in the turbine housing and will be based on an existing design from Hochschule Luzer in Zurich, Switzerland. They have a successful design in operation and have shared their drawings and experience for this project. Based on their good experience with the bearing block, the new design will be kept the same when suitable for our laboratory, though some modifications must be done.



(a) Old Bearing block when disassembled



(b) Turbine Housing without the bearing block

Figure 6.1: Old bearing block assembly.

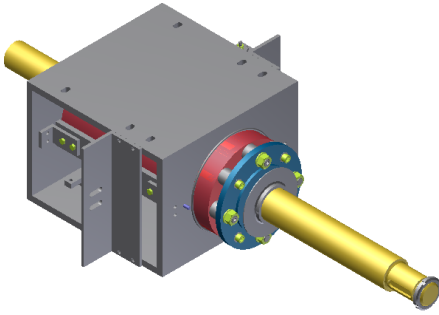


Figure 6.2: CAD drawing of the existing design.

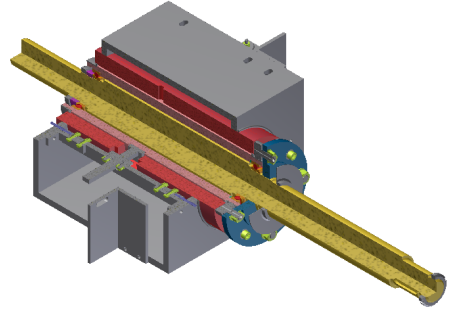


Figure 6.3: Section view of the existing design.

6.1 Bearing Concept

The basis for the new design is shown in figure 6.2. It is comprised of four main parts; the turbine shaft, an inner cylinder, an outer cylinder and the bearing casing. The turbine shaft is coupled to the inner cylinder with two roller bearings. The inner cylinder is in turn fixed to the outer cylinder with four roller bearings on each end and can rotate freely. This allows us to measure the friction torque by fixing the rotating inner cylinder to a force cell. Figure 6.4 shows the force cell bolted to the inner cylinder around the turbine shaft. Opposite of the force cell, a beam is bolted to the inner cylinder for calibrating the force cell. Figure 6.5 shows the roller bearings connecting the turbine shaft to the inner cylinder and the four roller bearings fixing the inner cylinder to the outer cylinder.

6.2 Bearing modifications

The bearing block is replacing an existing bearing configuration and must fit into the turbine test rig. Additionally it must be able to support the weight of the turbine runner and hydraulic forces without too much deflection. The system's resonant frequency should not match the frequency of the speed of rotation. Keeping the main dimension of the bearing block, the turbine shaft will be modified to meet the required maximum deflection and resonance frequency. A shaft diameter of 0.078m in the cantilever part is the highest possible to keep the original roller bearings and will therefore be set as a design parameter.

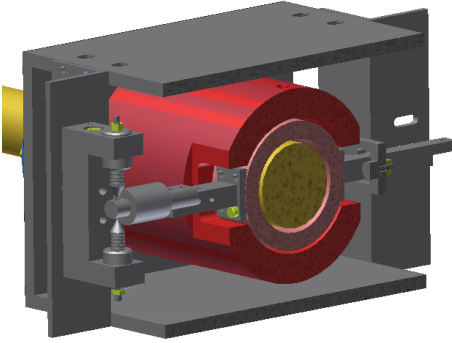


Figure 6.4: Method of calibrating and measuring the friction

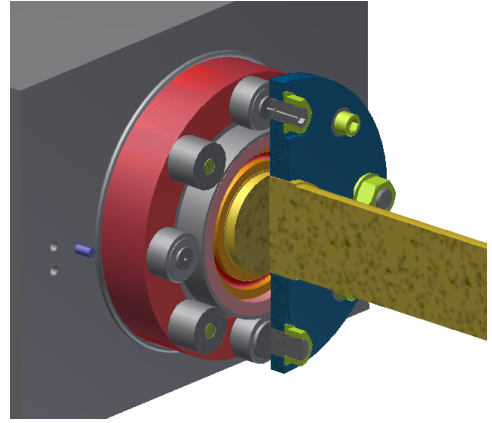


Figure 6.5: Section view of the bearings.

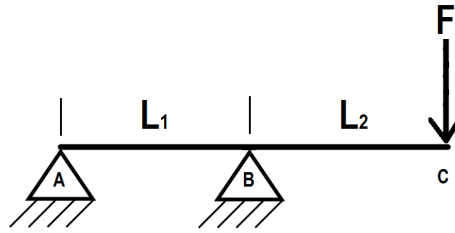


Figure 6.6: Model of the forces applied to the Turbine shaft

6.2.1 Maximum deflection

In discussion with Dahlhaug [6] the maximum allowed deflection of the turbine runner during operation was set to 1.00%.

The maximum total force applied to the turbine shaft can be calculated from the maximum capacity of the pump. The pump can deliver 100 l/s at a 100 m effective head. This amounts to a total force of just under 2500 N. The turbine shaft can be modeled as in figure 6.6 where point A and B represent the two roller bearings and point C is where the forces are applied to the turbine runner. The length of the cantilever section BC will need only to be 0.5 m or less.

The deflection will then be as superposition of a cantilever beam BC, with an applied force F and a simply supported beam, AB with a torque $M_B = FL_2$

applied to it in point B. The resulting deflection u_{tot} of point C is found from [7] equation 6.2.1 to be 0.1% Which is well within the requirement.

L_1	0.45	m
L_2	0.5	m
D_1	90	mm
D_2	78	mm
I_1	$1.82 \cdot 10^{-6}$	m^4
I_2	$3.22 \cdot 10^{-6}$	m^4
E	210	GPa

Figure 6.7: Shaft Properties

$$u_{tot} = u_{FC} + u_{MB} \quad (6.2.1.1)$$

$$u_{FC} = \frac{FL_2^3}{3EI} \quad (6.2.1.2)$$

$$u_{MB} = \frac{M_B L_1 L_2}{3EI} \quad (6.2.1.3)$$

6.2.2 Resonance

The fundamental frequency of a cantilever beam with end mass is given by equation 6.2.2.1 [8]:

$$f_1 = \frac{1}{2\pi} \sqrt{\frac{3EI}{(0.2235\rho L + m)L^3}} \quad (6.2.2.1)$$

where ρ is the mass per unit length and m is the mass on the end. The turbine shaft has mass per unit length of 38 kg/m and a constant weight of 20kg on the end plus the weight of the turbine runner. The runner weight varies from 7 to 25 kg. Depending on the length of the shaft, the fundamental frequency will range from 60 Hz for the longest shaft to 140 Hz for the shortest option. The forces from the water jet will have a frequency on the shaft depending on the rotational speed of the generator. This in turn depends on the diameter of the runner and the jet velocity.

The rotational speed of the turbine will be in the order of 1000 RPM or 20 Hz for the highest jet velocity and smallest wheels and will not interfere with the fundamental frequency. The frequency of the jet hitting the buckets will be more than 180 Hz and will not interfere with the fundamental frequency of the shaft. Resonance will not occur during tests and the length of the shaft can be chosen freely. A shortest shaft possible is therefore selected to maximize stability and minimize the tension on the shaft.

6.3 Water Control

The old bearing system used rubber seals to keep the water out of the bearings. For the new design it is important that there is no additional friction that can't be measured. A contactless seal is designed to keep the water from entering the bearings. A cylindrical cover shown in figure 6.9, is designed to keep most of the water away from the main shaft. Figure 6.8 shows the main shaft with three circular disks. The disks are designed to direct the water that enters away from the shaft by centrifugal forces. It will then be collected by the inside of the cover and fall to the bottom and exit through a slit and back into the turbine housing.

The eight holes seen at the end of the cover are there to fasten an end piece that fits the existing circular mounting disk used to fasten the turbine runner. If water surpasses the designed system, it can be checked by inspecting the inner cover from underneath the bearing block outside of the turbine housing.

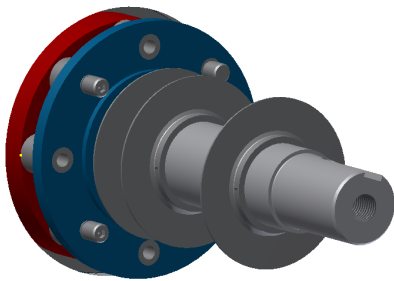


Figure 6.8: Three circular disks directing water away from the shaft.

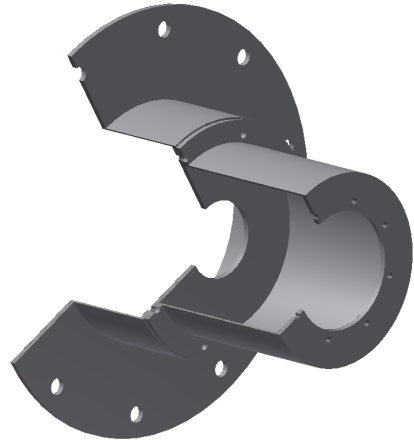


Figure 6.9: Three quarter section view of the cover.

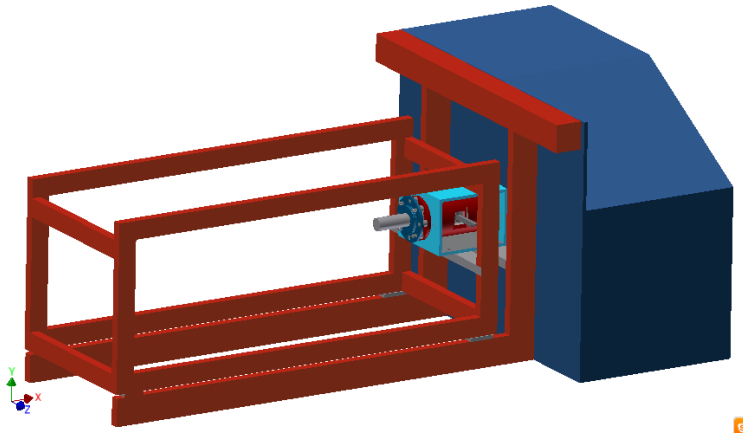


Figure 6.10: Bearing block placed on two beams

6.4 Installation

For the new bearing block to be installed, the old configuration must be disassembled and the test rig must undergo some modifications. The support for the old bearing system must be cut out to make room for the installment of the new bearing block. To support the new bearing block it is proposed to fit two new horizontal beams underneath it as showed in figure 6.10 in grey. The two beams will be supported by vertical supports to better hold its weight and to reduce vibrations.

6.5 Production

Machine drawings were made using Autodesk Inventor, though for some of the parts, the drawings were received from Zurich. The machine drawings are put in Appendix G, however, they are more easily studied digitally in PDF. The material and part's order lists are given in Appendix F. As far as time and tolerances permitted it, the parts were machined by the technicians at NTNU and only a few parts were made externally. The assembly, installation and fitting were done at the Water Power Laboratory.

Chapter 7

Results

In this chapter the test results from before and after the upgrade are presented. The results from the friction tests are given, and the finished test turbine is presented visually.

7.1 Efficiency

Figure 7.1(a) shows the complete hill diagram before upgrading. The efficiency shown is the total efficiency, η . This is due to the fact that the friction torque was not measured.

The best efficiency point recorded is $\eta = 89.40\%$ at $n_{ED} = 12.9$ and $Q_{ED} = 0.0056$.

Figure 7.1(b) shows the complete hill diagram after upgrading. After upgrading it was possible to measure both the hydraulic efficiency, η_h and the total efficiency, η .

The BEP recorded is $\eta_h = 90.75\%$ at $n_{ED} = 13.0$ and $Q_{ED} = 0.0056$.

The best total efficiency recorded for this run is $\eta = 90.13\%$.

7.1.1 Comparing the hydraulic and total efficiency

Figure 7.2 compares the hydraulic efficiency η_h after the upgrade with the total efficiency η before and after the upgrade. It shows how much impact the friction torque has on the total efficiency. The red and blue lines are done at the end of the day while the bearings were warm and show the hydraulic and total efficiency. The green line shows the total efficiency measured the next day when the test rig was cold and the black line is the total efficiency before upgrading.

In figure 7.3 the crossections of the two hill diagrams along constant Q_{ED} are shown. This gives the total and hydraulic efficiency before and after upgrading and it is given together with their respective total uncertainty.

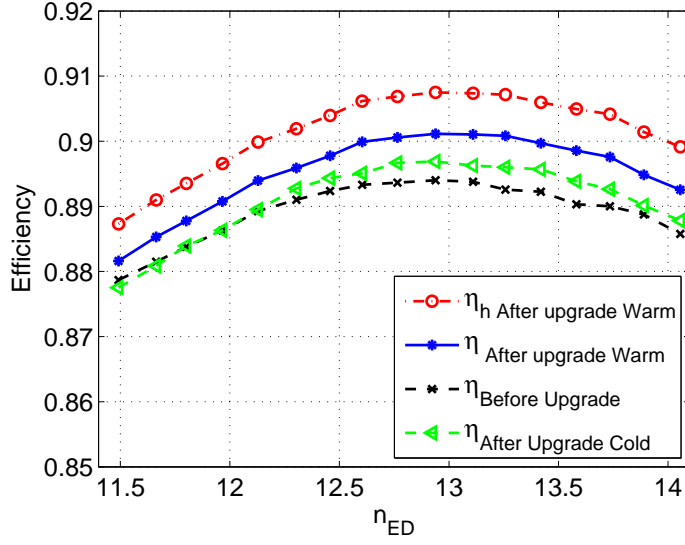


Figure 7.2: The graph shows the efficiency before and after upgrading, with and without the friction torque for constant volume flow.

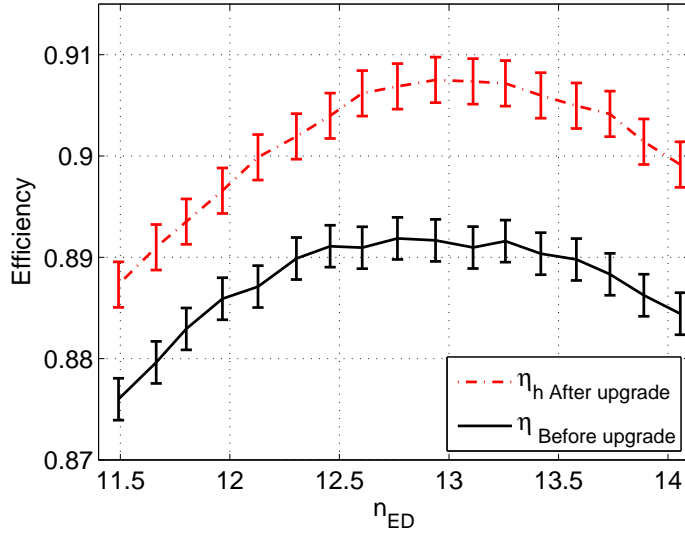
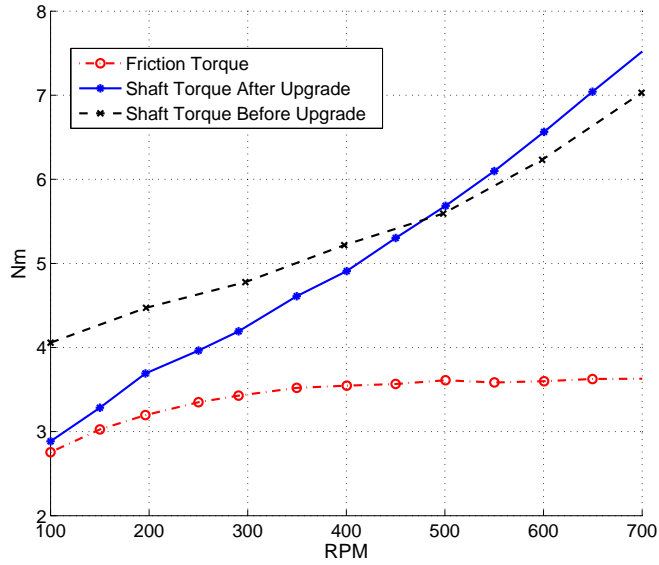


Figure 7.3: Efficiency curve with total uncertainties at best nozzle opening before and after upgrade.

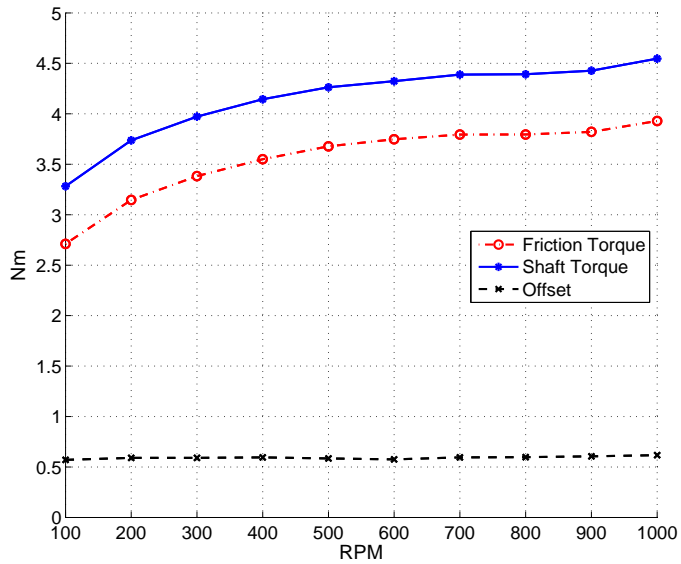
7.2 Friction Torque Verification

Figure 7.4(a) shows the torque needed to run the turbine runner without water for different speeds using the generator as a motor. The black line represents the shaft torque before the upgrade and the blue and red line represent the shaft and friction torque after the upgrade. Note that figure 7.4(a) shows no correlation between the friction torque and the shaft torque.

Figure 7.4(b) shows the same test without the turbine runner attached. The friction torque and shaft torque follow each other perfectly with a near constant offset shown with the black line.



(a) Friction torque as a function of rotational speed. Done with the runner attached before and after the upgrade



(b) Friction test without the runner done after the upgrade.

Figure 7.4: Friction torque tests performed without water.

7.3 Uncertainties and Repeatability

7.3.1 Uncertainties

Tables 7.1 and 7.2 show the relative uncertainties before and after the upgrade. Table 7.2 only includes the uncertainties that changed with the new bearing block. The total uncertainty is in this case calculated using the uncertainties from table 7.1 for hydraulic energy, discharge and rotational speed.

The uncertainties in discharge and torque consist of a constant part and a variable part. This is due to the variation in the uncertainties related to the regression process used in calibration.

Systematic:	Symbol	Constant [%]	Variable[%]	Total at BEP [%]
Hydraulic energy	f_{E_s}	0.03440	-	0.0344
Discharge	f_{Q_s}	0.09148	0.015-0.007	0.0919
Torque	f_{T_s}	0.08536	0.150-0.350	0.1992
Rotational Speed	f_{n_s}	0.0250	-	0.0250
Total Systematic:	f_{η_s}	-	-	0.2235
Total Random:	f_{η_r}	-	-	0.0111
Total:	f_{η_t}	-	-	0.2238

Table 7.1: Uncertainties before upgrade

Systematic	Symbol	Constant [%]	Variable[%]	Total at BP [%]
Shaft Torque	f_{T_s}	0.0854	0.17-0.39	0.2050
Friction Torque	$f_{T_{LM_s}}$	0.186	1.8-2.70	2.507
Total Torque	$f_{T_{tot_s}}$	-	-	0.2230
Total Systematic:	f_{η_s}	-	-	0.2450
Total Random:	f_{η_r}	-	-	0.0360
Total:	f_{η_t}	-	-	0.2476

Table 7.2: Uncertainties after upgrade

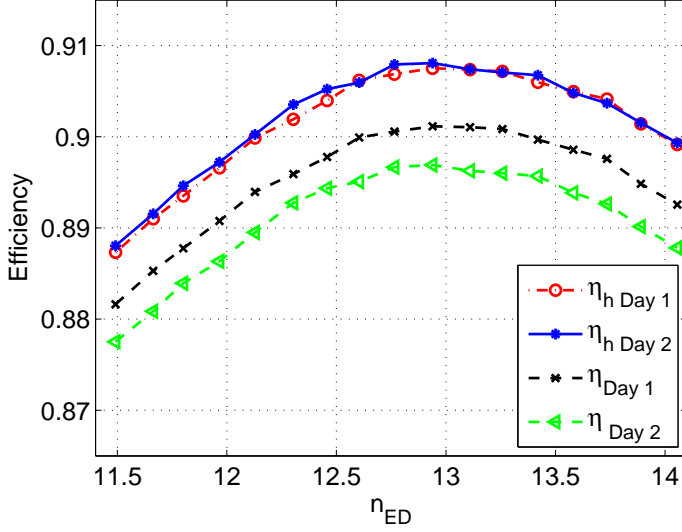


Figure 7.5: The graph shows the hydraulic and total efficiency recorded for 14mm nozzle opening on two different days.

Using the relative total uncertainties in tables 7.1 and 7.2 we get the efficiency before upgrading $\eta = 89.40 \pm 0.20\%$ and after upgrading, $\eta_h = 90.75 \pm 0.223\%$

7.3.2 Repeatability

To test the system's repeatability, i.e. the ability to produce the same results at the same operation points, two tests were done. Figure 7.5 shows the hydraulic efficiency η_h for constant nozzle opening and the corresponding total efficiency.

Figure 7.6 shows the results from running the same operation point every day for a week. As one can see, the recorded efficiency vary with 0.12% from maximum to minimum and $\pm 0.06\%$ from the mean.

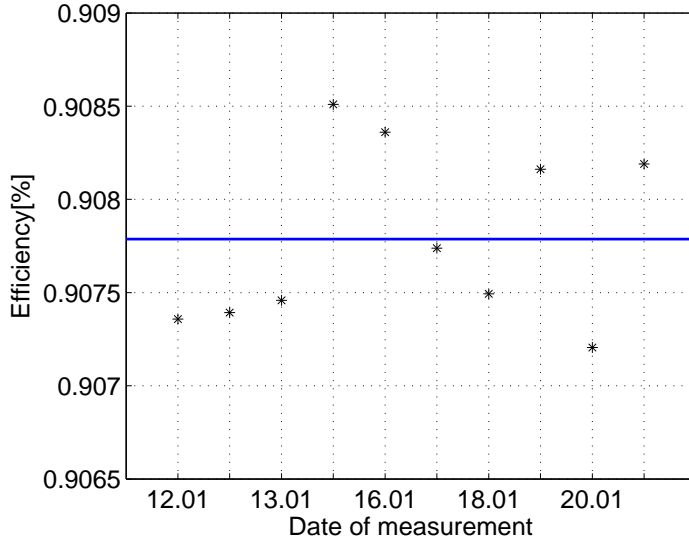
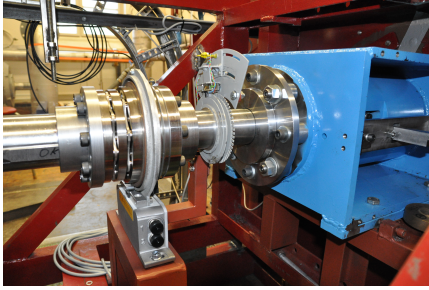


Figure 7.6: The graph shows the variation in measured efficiency at the same operation point on five days

7.4 New Test Rig

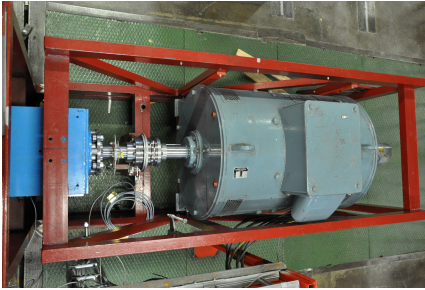
The pictures in figure 7.7 show the final product as it stands in the Water Power laboratory today. Figure 7.7(a) shows the new torque transducer and the rotational speed counter to the left of the bearing block. In figure 7.7(b) and 7.7(c) a clearer view of the test rig's arrangement is shown. The cover that was designed for keeping out water is shown in figure 7.7(d). Figure 7.7(e) and 7.7(f) shows the force cell measuring the friction and the lever arm for calibrating it.



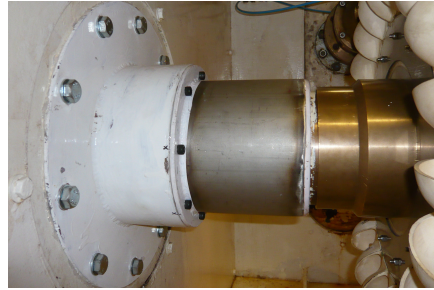
(a) Torque Transducer.



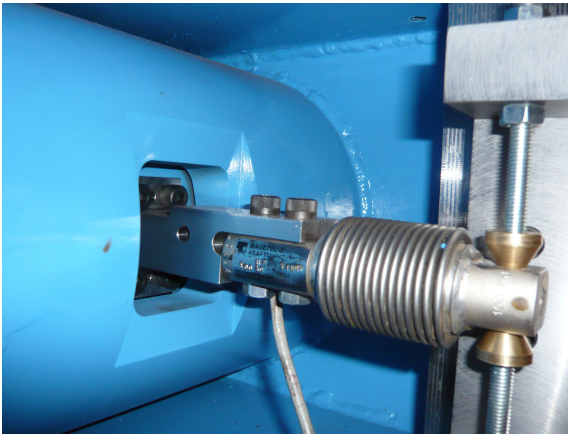
(b) Turbine Test Rig.



(c) Topview of generator and Bearing block.



(d) Cover.



(e) Force cell for friction torque.



(f) Lever arm and weight for calibrating.

Figure 7.7: Pictures of the upgraded test rig.

Chapter 8

Discussion

8.1 Efficiency

The efficiency before upgrading is consistent with tests done previously by Trefall [1]. The efficiency is slightly lower than what was obtained by Trefall, $\eta = 89.4\%$ compared to $\eta = 89.7\%$. This can be explained by the fact that Trefall's test was done with higher effective head which makes the friction losses smaller relative to the total mechanical power.

If we compare the hill diagrams in figure 7.1, a higher measured efficiency is found after upgrading. As expected, the hydraulic efficiency is higher than the total efficiency. This is shown even clearer in figure 7.2 where the hydraulic and total efficiency are shown together. Figure 7.3 further validates the importance of including the friction torque, and confirms friction to be the cause of higher efficiency and not uncertainty in the measurements. What is surprising is how much the friction torque varies. Comparing the blue and green line, we see an increase in efficiency of about half a percent due to less friction in the bearings when they are warm.

The most obvious difference, however, is how much smoother the hill diagram is in figure 7.1(b). As seen in figure 7.2, the friction torque varies substantially during the day. This could explain part of the roughness in figure 7.1(a). Another factor is the new torque transducer which is brand new and purchased exactly for this purpose.

8.2 Friction Torque Measurements

As mentioned in section 8.1, the friction torque varies as we run the test. It appears to go down as the temperature in the bearings go up. Such variation makes reliable measurements very important. Figure 7.4 shows the friction as a function of rotational speed. Figure 7.4(a) shows some similarity between the friction before upgrading and after, although the bearing system is very different. Finding that the blue and red graph on figure 7.4(a) showed little correlation, another test was done without the runner.

Figure 7.4(b) appears to validate the friction torque measurements. The measured friction torque and shaft torque follow each other nearly perfectly. The difference between the two is close to constant and showed in black. The source of this offset is believed to be the zero point calibration of the torque transducer which is calibrated in the range of 0-500 Nm. A more surprising aspect of the results showed in figure 7.4 is how much loss is produced by the runner. In the range of 600-700 RPM, which is the range in which the hill diagram was obtained, we see that the runner contributes to more friction than does the friction in the bearings.

8.3 Repeatability

Figure 7.5 shows the efficiencies both with and without friction torque included on two separate occasions. Despite the large difference in friction torque leading to the difference we see in total efficiency, the hydraulic efficiency stays the same. This shows the advantage of being able to measure the friction torque. To further test the repeatability, the same operational point was tested for several days keeping everything else constant. As shown in figure 7.6 the efficiency varies with only $\pm 0.06\%$ from the average from one day to the next. Even though it might look like much in the figure, it is substantially less than the systematic uncertainty of 0.245% . And considering that IEC [2] states that the random uncertainty in hydraulic efficiency should be no more than 0.1% , this small variation can be both expected and accepted. It is worth noticing, however, that the variation we see in figure 7.6 is not only due to random uncertainty in the measurements. As we see in table 7.2 the random uncertainty is only about 0.03% . The variation we see can come from the fact that the test rig is unable to hold an operation point absolutely constant. There are always variations in the head, discharge or the rotational speed of the turbine. This variation is believed to lead to the

inconsistency we see from one run to another.

8.4 Uncertainties

The uncertainties of the measurements before upgrading are less than what Trefall found with a total uncertainty of 0.2235 % at BEP. The uncertainty related to the torque measurements dominate the total uncertainty.

After upgrading, we have slightly higher systematic uncertainty. As for the uncertainty before the upgrade, we have the biggest uncertainty related to the torque measurements. Since the uncertainty related to the torque stems from the calibration process and the procedure for calibrating the torque transducers was identical in both cases, it is not surprising that the uncertainty remains more or less the same.

The uncertainty in the friction torque measurements, as for the shaft torque, stems from the calibration process. As this was a new measurement, a new procedure was created. It can be found in Appendix A. The limited selection of weights available resulted in a fairly high relative uncertainty in the friction torque. $f_{Lm_s} = 2.5\%$. But since the friction torque is only about one percent of the total torque, the absolute impact it has on the total uncertainty is only a tenth of that of the shaft torque.

Referring back to table 2.1, and comparing with table 7.1 and 7.2, we see that at BEP, all uncertainties are within the limits set by IEC.

Chapter 9

Conclusion

With the upgraded test rig, the efficiency of the reference runner was found to be $\eta_h = 90.75 \pm 0.223\%$, compared to $\eta = 89.40 \pm 0.20\%$ before upgrading. This means that more than one percent lost in the bearings, used to be unaccounted for. Although the total uncertainties were not found to be lower with the new system, the friction torque is now quantifiable. It is also found that the uncertainties are within the limits set by the IEC standard.

Upgrading the bearing block and the torque measurement system proved to be a success. With the new test rig it is now possible to measure the true hydraulic efficiency for Pelton turbines in the Water Power Laboratory. The turbine test rig operates as desired without problems. The measurements show good repeatability at all times and the friction measurements are shown to give reliable readings. Being able to measure the friction torque will make testing much more reliable in the future and is especially important when comparing models with small geometrical changes.

Bibliography

- [1] Stine Trefall. Modelltester av peltonturbiner ved vannkraftlaboratoriet, 2011.
- [2] IEC. *Hydraulic turbines, storage pumps and pump-turbine- Model acceptance tests*. International Electrotechnical Commission, 1999.
- [3] John Robert Taylor. *Introduction to Engineering Experimentation*. University Science Books, 1993. ISBN 0-07-063091-7.
- [4] Ye Warpole, Myers. *Probability and Statistics for Engineers and Scientists*. Pearson International Edition, 2007. ISBN 0-13-204767-5.
- [5] Pål-Tore Selbo Storli. Modelltest av francis turbin i vannkraftlaboratoriet. NTNU, 2006.
- [6] Ole Gunnar Dahlhaug. Personal correspondance, Fall 2011.
- [7] Fridtjov Irgens. *Formelsamling mekanikk*. Tapir akademisk forlag, Trondheim, 3, 3.rd print edition, 2005. ISBN 82-519-1506-6.
- [8] Tom Irvine. Bending frequencies of beams, rods, and pipes, April 2004. URL <http://www.vibrationdata.com/tutorials2/beam.pdf>.
- [9] Lars Fjærvold. Collaboration. NTNU, 2011.

Appendix A

Calibration of Friction Torque

This procedure describes how the force transducer used for measuring friction torque on the Pelton Turbine Test Rig is calibrated in the Hydropower Laboratory.

A.1 The system

A.1.1 Description

The system measuring the friction torque is shown in figure A.1. The main shaft is connected to an inner cylinder by two roller bearings and to the generator by two torque flanges. The inner cylinder can roll freely in the radial direction. It has an arm connected to it that will exert a force on the force cell. The force cell has a load capacity of 5 kg. Adjacent to the force cell there is an beam/level arm of length 0.25m used for calibrating the force cell. On this arm we will hang weights. Many factors will influence the force measured by the force cell. The stick friction in bearings and in the generator will give unaccurate readings during calibration. It is therefore necessary to take certain precautions described in section A.2.

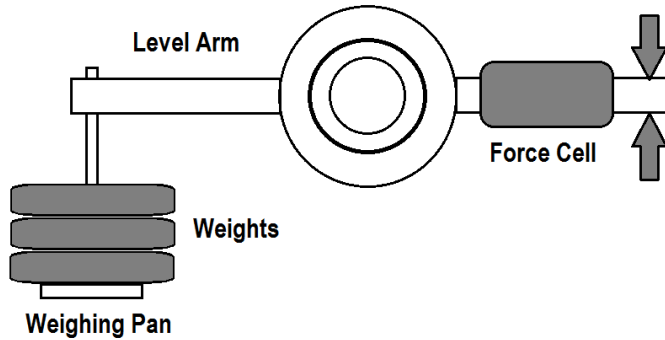


Figure A.1: Friction torque Calibration Setup

A.1.2 Equipment used in Calibration

- Weighing pan on which we put the weights
- Weights of 0.5 and 1 kg.
- General Calibration program in labview.

The weights are weighed in the laboratory and are numbered:

1. 976.0 g
2. 980.5 g
3. 976.0 g
4. 977.5 g
5. 978.0 g
6. 486.5 g
7. 488.5 g
8. Weighing pan: 140.0 g

A.2 Calibration

A.2.1 Preparation

1. Disconnect the HBM Torque transducer from the flange connected to the generator shaft and make sure there is no contact between the torque transducer and the flange.
2. Make sure the Force cell is tightly fastened in both ends.
3. Prepare the weights used for calibration.

A.2.2 Calibration

The zero point is set to have a constant offset using the weighing pan and a 1kg weight. This is done for stability purposes because of large fluctuations around the true zero point of the force cell. This weight will hang on the level arm always.

For calibration the weights are put on the weighing pan up to around 7 Nm additional load. Each point is logged in labview until a satisfying uncertainty is reached. The calibration points can be done as following:

Torque[Nm]	Volt[V]
0.000000	2.997640
1.194536	3.896813
2.393982	4.826799
4.803924	6.726423
5.998460	7.666758
7.197906	8.626601
7.197906	8.665635
5.998460	7.745306
4.803924	6.819931
2.407487	4.954879
0.000000	3.080269

Table A.1: Calibration Points

A.2.3 Note

A better calibration curve was observed when giving a light knock on the bearing block for every new load. This is to "reset" the stick friction in the 8 bearings holding the inner cylinder in place to get a more accurate reading. When running tests later, vibrations will do this for us.

Appendix B

Systematic Uncertainty Before Upgrade

In the proceeding section the uncertainties in the first setup will be explained and calculated. Then it will be summarized in the end.

B.1 Hydraulic energy E

The uncertainties in the calculation of the hydraulic energy are as follows:

$$f_E = \pm \frac{e_E}{E} = \pm \frac{\sqrt{(\frac{e_p}{\rho})^2 + (g \cdot e_{Z_{dif}})^2 + (\frac{e_{v_1^2}}{2})^2}}{\frac{p}{\rho} + g e_{Z_{dif}} + \frac{e_{v_1^2}}{2}} \quad (\text{B.1.0.1})$$

Being that the experiments are run on a pelton turbine which runs on high pressure and low volume flow, some simplifications can be justified. The total head of during the experiment is held constant at 70 m. The height difference between the pressure transducer and the inlet is measured to be 217 mm with a measurement uncertainty of 0.5 mm. The relative total uncertainty in hydraulic energy this error imposes on the total uncertainty is therefore:

$$\frac{e_{Z_{dif}}}{E} = \frac{0.0005m}{70m} = 0.00071\% \quad (\text{B.1.0.2})$$

Further we have the contribution of the error in inlet velocity to the total hydraulic efficiency. At the maximum nozzle opening we have a discharge of $0.45\text{m}^3/\text{s}$ which in a 100 mm pipe gives us a velocity of 5.7 m/s. This is a contribution of 1.7m or 2% to the total head at maximum flow. Although the uncertainty related to the discharge varies, when calculating the uncertainty in the inlet velocity v_1 , the maximum uncertainty in discharge is used.

$$\frac{e_{v_1^2}}{2} = v_1^2 \cdot f_{v_1} \quad (\text{B.1.0.3})$$

$$f_{v_1} = \sqrt{f_Q^2 + f_A^2} \quad (\text{B.1.0.4})$$

$e_{Z_{dif}} = 0.0005\text{m}\%$	Error is set to half of the resolution of the ruler.
$f_{p_{ab}} = 0.0008\%$	Found from the documentation of the dead weight manometer
$f_{p_{reg}} = 0.035\%$	Found from the calibration file for the range used in this test
$f_Q = 0.0926\%$	Highest systematic uncertainty in discharge during tests.
$f_{A_i} = 0.01\%$	Found from Storli [5]
$\Delta p = 670\text{kPa}$	The static pressure in front of the nozzle.
$v_1 = 5.7\text{m}$	The velocity of the water prior to the nozzle.
$E = g \cdot 70\text{m}$	The Hydraulic energy available before the nozzle.

$$f_E = \pm \frac{\sqrt{(\frac{f_p \cdot \Delta p}{\bar{p}})^2 + (g \cdot e_{Z_{dif}})^2 + (\frac{v_1^2 \cdot f_{v_1^2}}{2})^2}}{E} \quad (\text{B.1.0.5})$$

Using the values above and equation B.1.0.5 we find a total systematic uncertainty in the hydraulic energy to be: 0.0344%

B.2 Discharge Q

The uncertainties that constitutes the hydraulic energy are taken from Storli [5], except for $f_{Q,reg}$ which has been calculated based on the current calibration of the flow transducer. The uncertainties related to the regression process was calculated based on the raw data obtained during the calibration using the weighing tank. The uncertainty was calculated with help from matlab code programmed by Lars Fjærvold [9]

$$f_{Q_{cal}} = \pm \sqrt{(f_{\Delta m})^2 + (f_{div})^2 + (f_{\rho_m})^2 + (f_{\Delta m})_t^2 + (f_{div})_s^2 + (f_{Q,reg})^2} \quad (\text{B.2.0.6})$$

$$\begin{aligned} f_{\Delta m} & 0.05073\% \\ f_{div} & 0.05055\% \\ f_{\rho_m} & 0.01000\% \\ f_{\Delta m_r} & 0.00072\% \\ f_{div_r} & 0.05653 \end{aligned}$$

Total constant uncertainty is 0.09148%.

$f_{Q,reg}$ varies from 0.015-0.007% in our points of operation.

$$f_{Q,reg} = (3.395 \cdot 10^{-7} \cdot (Q \cdot 1000)^2 - 2.3697 \cdot 10^{-5} \cdot (Q \cdot 1000) + 3.4582 \cdot 10^{-3}) / (Q \cdot 1000) \cdot 100 \quad (\text{B.2.0.7})$$

B.3 Torque

The systematic uncertainty of the torque measurements is related to the calibration of the torque transducers.

$$f_{T_{cal}} = \pm \sqrt{(f_{\tau W})^2 + (f_{\tau arm})^2 + (f_{\tau_{reg}})^2 + (f_{\tau_{friction}})^2} \quad (\text{B.3.0.8})$$

$f_{\tau W}$ is the uncertainty in the mass of the calibrated weights. The same weights were used by Storli [5] and the uncertainty found to be 0.00154%.

$f_{\tau arm}$ is the uncertainty in the measured length of the level arm. The arm was measured to be 1.10515 m consisting of two measurements; the length of the arm $L = 1.070 \pm 0.005$ and the diameter of the shaft $D = 0.07015 \pm 0.00005$.

$$f_{\tau arm} = \sqrt{f_L^2 + f_D^2} = 0.08536\% \quad (\text{B.3.0.9})$$

$$\begin{aligned} f_{\tau W} & 0.00154\% \\ f_{\tau arm} & 0.08536\% \\ f_{\tau_{reg}} & y = -0.9798E-08 * M^3 + 1.3044E-05 * M^2 - 0.00565863 * M + .953585 \\ f_{\tau_{friction}} & \text{Uncertainty in the measurement of the friction torque. Does not apply for the first setup} \end{aligned}$$

Total constant systematic uncertainty: 0.08536% Total variable systematic uncertainty: 0.15% -0.35%

B.4 Summary of Uncertainties

Systematic uncertainties:

Measurement	Symbol	Constant [%]	Variable[%]	Total at BP [%]
Hydraulic energy	f_{E_s}	0.03440	-	0.0344
Discharge	f_{Q_s}	0.09148	0.015-0.007	0.0919
Torque	f_{T_s}	0.08536	0.150-0.350	0.1992
Rotational Speed	f_{n_s}	0.0250	-	0.0250
Total:	f_{η_s}	-	-	0.2235

Table B.1: Uncertainties before upgrade

Appendix C

Systematic Uncertainty After Upgrade

All that has changed after upgrading to the new test rig is the way we measure the torque. Therefore for our purposes the uncertainty related to the torque is all we are interested in.

C.1 Torque

C.1.1 Shaft torque

Since the shaft torque is measured the same way as before, the same uncertainties will be the same except for the uncertainties related to the regression process used in calibration.

The calibration is done with the same equipment as before so the constant part of the uncertainties like the uncertainty in the measurement of the lever arm will stay the same.

From the calibration data E we see that the uncertainty related to the regression process varies between 0.17-0.37% in the range of 155-450 Nm torque. In addition we have a constant part that we can find from the first uncertainty analysis. This is 0.08536%

At BEP we have a torque of 280 Nm giving a total systematic uncertainty of $f_{T_s} = \sqrt{0.187^2 + 0.0854} = 0,205\%$ or 0.574Nm.

C.1.2 Friction Torque

The systematic uncertainty in the friction torque measurements is related to the calibration of the force cell.

$$f_{T_{Lm_{cal}}} = \pm \sqrt{(f_{\tau W})^2 + (f_{\tau arm})^2 + (f_{\tau reg})^2} \quad (C.1.2.1)$$

$f_{\tau W}$ is the uncertainty in the mass of the weights used for calibration. The weights were custom made and weighed in the laboratory. The scale used has an uncertainty of 0.5 g. The uncertainty is therefore found to be 0.11%.

$f_{\tau arm}$ is the uncertainty in the length of the level arm. The arm was machined to be 180mm with an uncertainty of 0.1mm. The inner cylinder on which the arm is connected was machined to be 70mm with an uncertainty of 0.1mm.

$$f_{\tau arm} = \sqrt{f_L^2 + f_D^2} = 0.15\% \quad (C.1.2.2)$$

$$f_{\tau W}=0.11\% \quad f_{\tau arm}=0.15\% \quad f_{\tau reg}=2.5\%$$

$f_{\tau reg}$ is found from E constant at its maximum at 2.5% within our range of operation.

Total systematic uncertainty: 2.5% At best point this amounts to 0.05 Nm absolute error in the torque measurements: $e_{T_{Lm}}$.

C.1.3 Mechanical Torque

The uncertainty in the total measured mechanical torque for the best efficiency point.

$$f_{T_m} = \frac{(e_{T_{Lm}})^2 + e_T^2}{T_{tot}} = \frac{0.05Nm + 0.574Nm}{280Nm} = 0.223\% \quad (\text{C.1.3.1})$$

Measurement	Symbol	Constant [%]	Variable[%]	Total at BP [%]
Shaft Torque	f_{T_s}	0.854	0.17-0.39	0.205
Friction Torque	$f_{T_{LMs}}$	0.187	1.8-2.7	2.506
Total Torque	$f_{T_{tot_s}}$	-	-	0.223

Table C.1: Uncertainties after upgrade

Appendix D

Calibration Data Before Upgrading

In this chapter all the calibration data for the first tests can be found.

They are put in this order:

1. Shaft Torque
2. Pressure
3. Flow

CALIBRATION REPORT

CALIBRATION PROPERTIES

Calibrated by: Kyrre Reinertsen, Lorentz Fjellanger Barstad
Type/Producer: Druck PTX 1830
SN: 2867610
Range: 0-500 Nm a
Unit: Nm

CALIBRATION SOURCE PROPERTIES

Type/Producer: Torque Transducer HBM T22
SN: 66256
Uncertainty [%]: 0,01

POLY FIT EQUATION:

$Y = + 7.45992138E+0X^0 - 100.16865016E+0X^1$

CALIBRATION SUMMARY:

Max Uncertainty : Inf [%]
Max Uncertainty : 0.888419 [Nm]
RSQ : 0.999958
Calibration points : 29

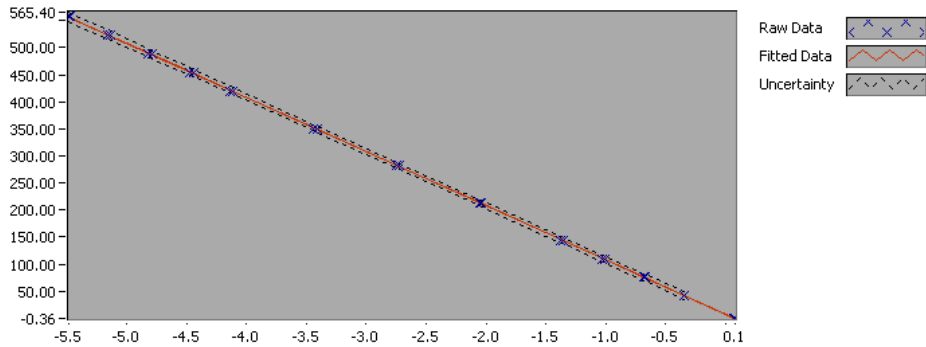


Figure 1 : Calibration chart (The uncertainty band is multiplied by 10)

Kyrre Reinertsen, Lorentz Fjellanger Barstad

CALIBRATION VALUES

Value [Nm]	Voltage [V]	Best Poly Fit [Nm]	Deviation [Nm]	Uncertainty [%]	Uncertainty [Nm]
0.000000	0.077754	-0.328591	0.328591	Inf	NaN
0.000000	0.078088	-0.362069	0.362069	Inf	NaN
41.277552	-0.343444	41.862264	-0.584712	1.707971	0.705008
75.652002	-0.668178	74.390429	1.261573	0.860143	0.650715
110.026933	-1.010013	108.631605	1.395327	0.549161	0.604225
144.401107	-1.355138	143.202269	1.198838	0.391941	0.565966
213.146363	-2.040516	211.855658	1.290705	0.239067	0.509562
281.901931	-2.723963	280.315640	1.586290	0.181267	0.510994
350.651586	-3.403392	348.373149	2.278437	0.157842	0.553476
419.403785	-4.111751	419.328478	0.075307	0.152573	0.639898
453.776654	-4.442535	452.462656	1.313998	0.156131	0.708485
488.149385	-4.783741	486.640796	1.508589	0.155398	0.758572
522.522803	-5.131920	521.517387	1.005416	0.159366	0.832725
556.896496	-5.467248	555.106774	1.789722	0.159071	0.885860
556.896496	-5.481271	556.511438	0.385058	0.159530	0.888419
522.522803	-5.157468	524.076538	-1.553735	0.157609	0.823545
488.149385	-4.821851	490.458224	-2.308839	0.155558	0.759357
453.776654	-4.477711	455.986158	-2.209504	0.153607	0.697034
419.403785	-4.136303	421.787788	-2.384003	0.152784	0.640781
350.651586	-3.439822	352.022261	-1.370675	0.155557	0.545462
281.901931	-2.749116	282.835207	-0.933277	0.176388	0.497242
213.146363	-2.054198	213.226206	-0.079843	0.232515	0.495597
144.401107	-1.376458	145.337819	-0.936712	0.386481	0.558083
110.026933	-1.030316	110.665265	-0.638332	0.546388	0.601174
75.652002	-0.686510	76.226694	-0.574692	0.855748	0.647390
41.277552	-0.342827	41.800456	-0.522904	1.707634	0.704869
0.000000	0.069513	0.496899	-0.496899	Inf	NaN
0.000000	0.069070	0.541307	-0.541307	Inf	NaN
0.000000	0.068040	0.644486	-0.644486	Inf	NaN

COMMENTS:

The uncertainty is calculated with 95% confidence. The uncertainty includes the randomness in the calibrated instrument during the calibration, systematic uncertainty in the instrument or property which the instrument under calibration is compared with (dead weight manometer, calibrated weights etc.), and due to regression analysis to fit the calibration points to a linear calibration equation. The calculated uncertainty can be used as the total systematic uncertainty of the calibrated instrument with the given calibration equation.

CALIBRATION REPORT

CALIBRATION PROPERTIES

Calibrated by: Kyrre Reinertsen, Lorentz Fjellanger Barstad
Type/Producer: Druck PTX 1830
SN: 2867610
Range: 0-10 bar a
Unit: kPa

CALIBRATION SOURCE PROPERTIES

Type/Producer: Pressurements deadweight tester P3223-1
SN: 66256
Uncertainty [%]: 0,01

POLY FIT EQUATION:

$Y = -403.42790854E+0X^0 + 199.64449144E+0X^1$

CALIBRATION SUMMARY:

Max Uncertainty : 35.384341 [%]
Max Uncertainty : 0.346930 [kPa]
RSQ : 0.999999
Calibration points : 30

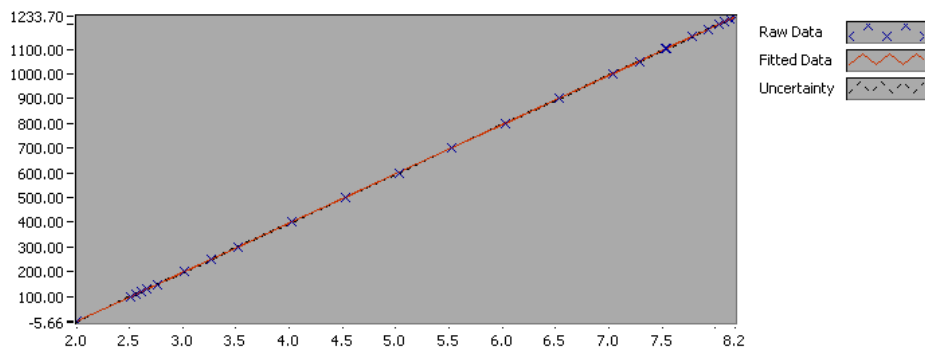


Figure 1 : Calibration chart (The uncertainty band is multiplied by 10)

Kyrre Reinertsen, Lorentz Fjellanger Barstad

CALIBRATION VALUES

Value [kPa]	Voltage [V]	Best Poly Fit [kPa]	Deviation [kPa]	Uncertainty [%]	Uncertainty [kPa]
-0.980461	2.009742	-2.193987	1.213526	35.384341	-0.346930
99.170610	2.515055	98.689032	0.481578	0.315402	0.312786
109.185717	2.565632	108.786413	0.399304	0.283412	0.309446
119.200824	2.616025	118.847055	0.353769	0.257069	0.306428
129.215931	2.666865	128.997056	0.218875	0.234613	0.303157
149.246145	2.767314	149.051089	0.195057	0.198712	0.296571
199.321681	3.019352	199.369145	-0.047465	0.141101	0.281245
249.397216	3.270705	249.550239	-0.153023	0.106902	0.266610
299.472752	3.522598	299.839359	-0.366607	0.084547	0.253196
399.623823	4.025179	400.176877	-0.553055	0.057666	0.230448
499.774894	4.527315	500.425509	-0.650615	0.043018	0.214993
599.925965	5.029350	600.654213	-0.728249	0.034241	0.205422
700.077035	5.531053	700.816405	-0.739369	0.029547	0.206848
800.228106	6.032862	800.999674	-0.771568	0.027255	0.218101
900.379177	6.533064	900.862387	-0.483209	0.026206	0.235951
1000.530248	7.033324	1000.736407	-0.206159	0.025644	0.256574
1050.605784	7.284068	1050.796159	-0.190375	0.025781	0.270854
1100.681319	7.533819	1100.657654	0.023665	0.026131	0.287614
1150.756855	7.783418	1150.488585	0.268269	0.026448	0.304348
1180.802176	7.933830	1180.517544	0.284632	0.026914	0.317805
1200.832390	8.033603	1200.436695	0.395695	0.026946	0.323578
1210.847497	8.084085	1210.515218	0.332279	0.026740	0.323785
1220.862604	8.133624	1220.405399	0.457205	0.027110	0.330973
1230.877711	8.183574	1230.377508	0.500203	0.026973	0.332008
1230.877711	8.182935	1230.249927	0.627785	0.027102	0.333594
1200.832390	8.033533	1200.422766	0.409624	0.026669	0.320249
1100.681319	7.535151	1100.923530	-0.242211	0.026270	0.289145
599.925965	5.031897	601.162697	-1.236733	0.034367	0.206177
99.170610	2.519588	99.593902	-0.423292	0.314965	0.312353
-0.980461	2.012663	-1.610925	0.630464	35.363345	-0.346724

COMMENTS:

The uncertainty is calculated with 95% confidence. The uncertainty includes the randomness in the calibrated instrument during the calibration, systematic uncertainty in the instrument or property which the instrument under calibration is compared with (dead weight manometer, calibrated weights etc.), and due to regression analysis to fit the calibration points to a linear calibration equation. The calculated uncertainty can be used as the total systematic uncertainty of the calibrated instrument with the given calibration equation.



NTNU

WATERPOWER LABORATORY NTNU

Calibration Sheet

Calibration of flow meter

Date:

15.05.07

Sign operator:

Approved:

Calibrator: Weighing tank system

Unit: Flowmeter, reg nr. 4624-4

Calibration constants
for weighing tank
correction

a ₁	4.00E-22
a ₂	-6.00E-17
a ₃	3.00E-12
a ₄	-1.00E-07
a ₅	1.00E+00

Corrected weight is calculated from formula
where parameters a,b,c,d and e is achieved
through substitution calibration.

$$W = a \cdot \frac{mW^5}{5} + b \cdot \frac{mW^4}{4} + c \cdot \frac{mW^3}{3} + d \cdot \frac{mW^2}{2} + e \cdot mW$$

Density of water is calculated from formula

$$\rho_w = \frac{1000}{(1 - 4,6999 \cdot 10^{-10} \cdot p_{abs}) + 8 \cdot 10^{-9} \cdot (\theta - 4 + 2,1318913 \cdot 10^{-5} \cdot p_{abs}) - 6 \cdot 10^{-9} \cdot (\theta - 4 + 2,1318913 \cdot 10^{-5} \cdot p_{abs})^2}$$

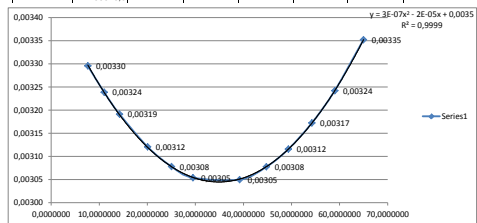
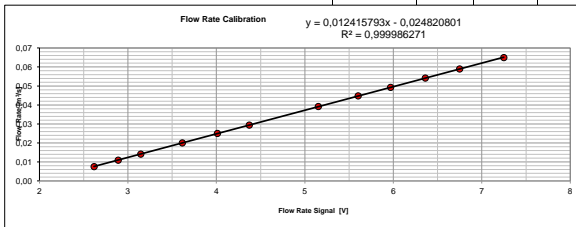
Density of air is calculated from formula

$$\rho_a = \frac{(p_{abs} \cdot 3,4837 \cdot 10^{-3})}{(273,15 + \theta)}$$

Discharge is found from formula

$$Q = \frac{W_1 - W_2}{\rho_w \cdot t \cdot (1 - \frac{\rho_a}{\rho_w})}$$

Time	Manual Observation before Weight	Manual Observation after Weight	Manual Observation Q	Manual Observation Q	Time	Ambient pressure P _{amb}	Water temp T _w	Air temp T _a	Calculated value before Weight	Calculated value after Weight	Differential weight	Density of water	Density of air	Differential volume	Calculated Flow Rate Q	Estimate Q	Deviation
	[kg]	[kg]	[m³/s]	[m³/s]		[kPa]	[°C]	[°C]	[kg]	[kg]	[kg]	[kg/m³]	[kg/m³]	[m³]	[m³/s]	[m³/s]	[%]
05.12.2011	16475.4	17389.0		2,516768	120.103	96.580	15,26	18,7	16465.3	17377.9	812.6	999.1131	1.1536	0,91447	0,00767	0,00767	0,70968
05.12.2012	17389.0	18711.0		2,889827	120.103	96.580	15,24	18,7	17377.9	18698.4	1320.5	999.1131	1.1536	1,32320	0,0110172	0,01106	0,37543
05.12.2013	18711.0	20416.9		3,145671	120.102	96.580	15,25	18,7	18698.4	20402.2	1703.9	999.1162	1.1536	1,70733	0,0142167	0,01424	0,13700
05.12.2014	20416.9	22823.4		3,614774	120.103	96.580	15,25	18,7	20402.2	22805.7	2403.4	999.1146	1.1536	2,40333	0,0202522	0,02036	0,03614
05.12.2015	22823.4	25827.5		4,012492	120.103	96.580	15,24	18,7	22805.7	25805.6	3000.0	999.1146	1.1536	3,00608	0,0250292	0,02500	-0,12690
05.12.2016	25827.5	29366.2		4,371142	120.103	96.580	15,29	18,7	25805.6	29339.0	3533.4	999.1052	1.1536	3,54063	0,0294799	0,02945	-0,10036
05.12.2017	29366.2	34072.4		5,151503	120.103	96.580	15,28	18,7	29339.0	34037.4	4698.4	999.1083	1.1536	4,70900	0,0391997	0,03914	-0,15452
05.12.2018	34072.4	39446.9		5,601617	120.103	96.580	15,31	18,7	34037.4	39403.8	5366.4	999.1162	1.1536	5,37739	0,0447731	0,04473	-0,10150
05.12.2019	39446.9	45376.9		5,968647	120.103	96.580	15,31	18,7	39403.8	45319.2	5915.4	999.1099	1.1536	5,92749	0,0493534	0,04928	-0,13946
05.12.2020	45376.9	51892.4		6,362261	120.103	96.580	15,31	18,7	45319.2	51818.8	6499.7	999.1052	1.1536	6,51300	0,0542284	0,05417	-0,10487
05.12.2021	51892.4	58983.1		6,748915	120.103	96.580	15,33	18,7	51818.8	58889.9	7071.1	999.1052	1.1536	7,08660	0,0592663	0,05927	-0,00014
05.12.2022	58983.1	66796.3		7,248911	120.103	96.580	15,38	18,7	58889.9	66679.0	7789.1	999.1052	1.1536	7,80509	0,0649866	0,06518	0,29696



Appendix E

Calibration Data After upgrade

In this chapter all the calibration data for the tests after upgrading are found.

They are put in the following order:

1. Shaft Torque
2. Friction Torque
3. Pressure
4. Flow

CALIBRATION REPORT

CALIBRATION PROPERTIES

Calibrated by: Kyrre Reinertsen
Type/Producer: HBM T12
SN: 0
Range: 0- 500 Nm
Unit: Nm

CALIBRATION SOURCE PROPERTIES

Type/Producer: Torque Transducer HBM
SN:
Uncertainty [%]: 0,01

POLY FIT EQUATION:

$Y = -8.27189283E+0X^0 - 50.29384590E+0X^1$

CALIBRATION SUMARY:

Max Uncertainty : Inf [%]
Max Uncertainty : 0.897014 [Nm]
RSQ : 0.999948
Calibration points : 24

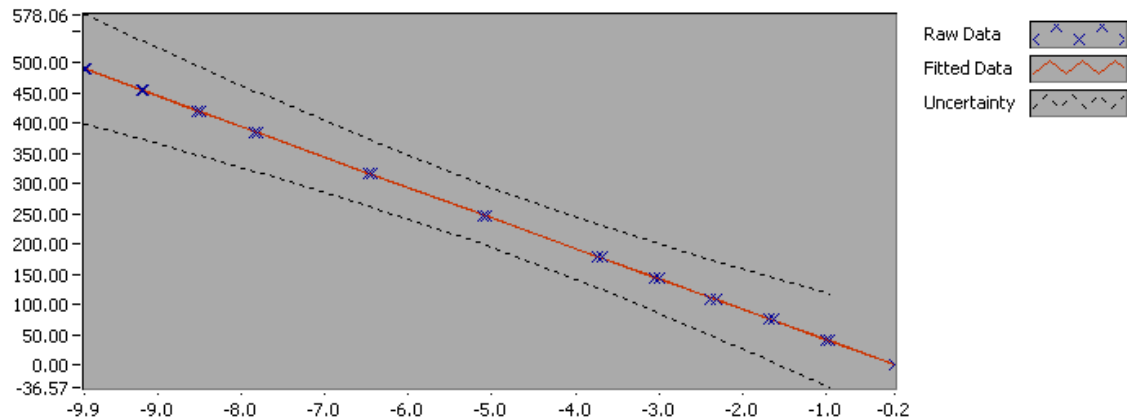


Figure 1 : Calibration chart (The uncertainty band is multiplied by 100)

Kyrre Reinertsen

CALIBRATION VALUES

Value [Nm]	Voltage [V]	Best Poly Fit [Nm]	Deviation [Nm]	Uncertainty [%]	Uncertainty [Nm]
0.000000	-0.181297	0.846250	-0.846250	Inf	NaN
41.277552	-0.968514	40.438419	0.839134	1.865742	0.770133
75.652002	-1.626942	73.553269	2.098733	0.920328	0.696246
110.026933	-2.310786	107.946411	2.080522	0.570078	0.627240
144.401107	-2.999079	142.563321	1.837786	0.393591	0.568350
178.771157	-3.686281	177.125373	1.645784	0.293203	0.524163
247.522875	-5.062089	246.320040	1.202835	0.198642	0.491683
316.276724	-6.430364	315.135840	1.140884	0.171414	0.542144
385.028854	-7.806436	384.343802	0.685052	0.170938	0.658160
419.403785	-8.493721	418.909994	0.493791	0.174344	0.731206
453.776654	-9.179876	453.419387	0.357267	0.178685	0.810831
488.149385	-9.863917	487.822428	0.326956	0.183348	0.895013
488.149385	-9.874545	488.356964	-0.207580	0.183758	0.897014
453.776654	-9.198805	454.371384	-0.594731	0.179246	0.813377
419.403785	-8.519852	420.224253	-0.820468	0.175141	0.734548
385.028854	-7.838560	385.959434	-0.930580	0.171998	0.662242
316.276724	-6.475454	317.403608	-1.126884	0.172447	0.545409
247.522875	-5.106809	248.569183	-1.046308	0.198632	0.491659
178.771157	-3.742785	179.967156	-1.195999	0.291817	0.521684
144.401107	-3.063089	145.782634	-1.381526	0.390218	0.563479
110.026933	-2.381710	111.513476	-1.486543	0.564061	0.620619
75.652002	-1.693694	76.910498	-1.258496	0.911086	0.689255
41.277552	-1.003975	42.221848	-0.944295	1.855522	0.765914
0.000000	-0.181751	0.869082	-0.869082	Inf	NaN

COMMENTS:

The uncertainty is calculated with 95% confidence. The uncertainty includes the randomness in the calibrated instrument during the calibration, systematic uncertainty in the instrument or property which the instrument under calibration is compared with (dead weight manometer, calibrated weights etc.), and due to regression analysis to fit the calibration points to a linear calibration equation. The calculated uncertainty can be used as the total systematic uncertainty of the calibrated instrument with the given calibration equation.

CALIBRATION REPORT

CALIBRATION PROPERTIES

Calibrated by: Kyrre Reinertsen
Type/Producer: HBM
SN: 0
Range: 0- 10 Nm
Unit: Nm

CALIBRATION SOURCE PROPERTIES

Type/Producer: Load Beam Force Cell Z6 HBM
SN:
Uncertainty [%]: 0,01

POLY FIT EQUATION:

$Y = -3.85451412E+0X^0 + 1.27859426E+0X^1$

CALIBRATION SUMARY:

Max Uncertainty : Inf [%]
Max Uncertainty : 0.062220 [Nm]
RSQ : 0.999506
Calibration points : 11

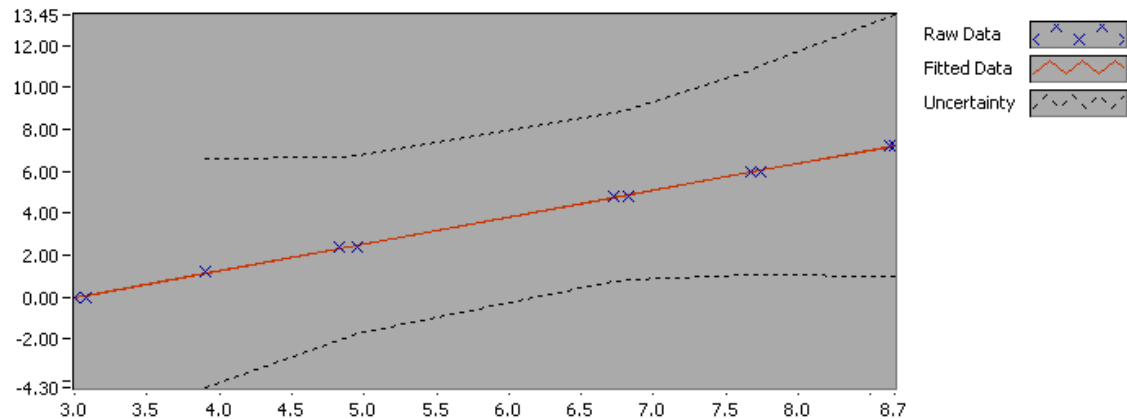


Figure 1 : Calibration chart (The uncertainty band is multiplied by 100)

Kyrre Reinertsen

CALIBRATION VALUES

Value [Nm]	Voltage [V]	Best Poly Fit [Nm]	Deviation [Nm]	Uncertainty [%]	Uncertainty [Nm]
0.000000	2.997640	-0.021749	0.021749	Inf	NaN
1.194536	3.896813	1.127928	0.066607	4.546208	0.054306
2.393982	4.826799	2.317003	0.076979	1.820209	0.043575
4.803924	6.726423	4.745852	0.058073	0.834093	0.040069
5.998460	7.666758	5.948158	0.050301	0.813391	0.048791
7.197906	8.626601	7.175408	0.022498	0.856430	0.061645
7.197906	8.665635	7.225317	-0.027411	0.864413	0.062220
5.998460	7.745306	6.048589	-0.050129	0.829013	0.049728
4.803924	6.819931	4.865411	-0.061487	0.846927	0.040686
2.407487	4.954879	2.480766	-0.073279	1.762693	0.042437
0.000000	3.080269	0.083900	-0.083900	Inf	NaN

COMMENTS:

The uncertainty is calculated with 95% confidence. The uncertainty includes the randomness in the calibrated instrument during the calibration, systematic uncertainty in the instrument or property which the instrument under calibration is compared with (dead weight manometer, calibrated weights etc.), and due to regression analysis to fit the calibration points to a linear calibration equation. The calculated uncertainty can be used as the total systematic uncertainty of the calibrated instrument with the given calibration equation.

CALIBRATION REPORT

CALIBRATION PROPERTIES

Calibrated by: Kyrre Reinertsen/ Christoph Imler
Type/Producer: Druck PTX 1830
SN: 2867610
Range: 0-12 bar a
Unit: kPa

CALIBRATION SOURCE PROPERTIES

Type/Producer: Pressurements deadweight tester P3223-1
SN: 66256
Uncertainty [%]: 0,01

POLY FIT EQUATION:

$Y = -402.61664267E+0X^0 + 199.49146048E+0X^1$

CALIBRATION SUMMARY:

Max Uncertainty : Inf [%]
Max Uncertainty : 0.392586 [kPa]
RSQ : 0.999999
Calibration points : 27

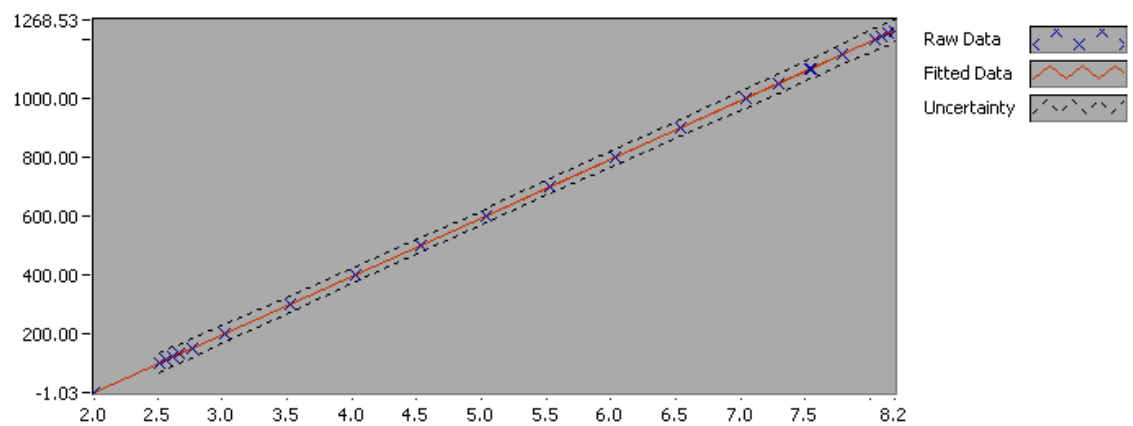


Figure 1 : Calibration chart (The uncertainty band is multiplied by 100)


Kyrre Reinertsen/ Christoph Imler

CALIBRATION VALUES

Value [kPa]	Voltage [V]	Best Poly Fit [kPa]	Deviation [kPa]	Uncertainty [%]	Uncertainty [kPa]
0.000000	2.013049	-1.030501	1.030501	Inf	NaN
100.151071	2.517959	99.694622	0.456449	0.333827	0.334331
110.166178	2.568967	109.870399	0.295779	0.300103	0.330612
120.181285	2.619464	119.944071	0.237214	0.271869	0.326736
130.196392	2.669755	129.976698	0.219694	0.248582	0.323645
150.226606	2.771363	150.246676	-0.020070	0.210888	0.316810
200.302142	3.022493	200.344859	-0.042717	0.153594	0.307652
300.453213	3.525990	300.788170	-0.334957	0.090968	0.273316
400.604284	4.029487	401.231666	-0.627382	0.063228	0.253292
500.755355	4.532428	501.564060	-0.808705	0.047282	0.236765
600.906426	5.034206	601.664399	-0.757974	0.038670	0.232371
701.057497	5.536129	701.793812	-0.736315	0.034021	0.238509
801.208568	6.037798	801.872546	-0.663978	0.033111	0.265284
901.359639	6.539663	901.990181	-0.630542	0.031730	0.286003
1001.510710	7.039768	1001.756999	-0.246289	0.032154	0.322024
1051.586245	7.290306	1051.737103	-0.150858	0.030778	0.323657
1101.661781	7.541448	1101.837829	-0.176048	0.030019	0.330705
1151.737316	7.790915	1151.604333	0.132983	0.030259	0.348505
1201.812851	8.039906	1201.275965	0.536886	0.032644	0.392316
1211.827959	8.089246	1211.118954	0.709005	0.030598	0.370799
1221.843066	8.140267	1221.297102	0.545963	0.032131	0.392586
1231.858173	8.189953	1231.209113	0.649060	0.030299	0.373239
1201.812851	8.040334	1201.361345	0.451507	0.030824	0.370453
1101.661781	7.539334	1101.416066	0.245715	0.031549	0.347564
600.906426	5.035618	601.946109	-1.039683	0.039441	0.237006
100.151071	2.520264	100.154555	-0.003484	0.337941	0.338451
0.000000	2.014564	-0.728247	0.728247	Inf	NaN

COMMENTS:

The uncertainty is calculated with 95% confidence. The uncertainty includes the randomness in the calibrated instrument during the calibration, systematic uncertainty in the instrument or property which the instrument under calibration is compared with (dead weight manometer, calibrated weights etc.), and due to regression analysis to fit the calibration points to a linear calibration equation. The calculated uncertainty can be used as the total systematic uncertainty of the calibrated instrument with the given calibration equation.

	WATERPOWER LABORATORY NTNU	Date: 15.05.07
	Calibration Sheet	Sign operator:
	Calibration of flow meter	Approved:

Calibrator: Weighing tank system

Unit: Flowmeter, reg nr. 4624-4

Calibration constants for weighing tank correction	a_1	4,00E-22
	a_2	-6,00E-17
	a_3	3,00E-12
	a_4	-1,00E-07
	a_5	1,00E+00

Corrected weight is calculated from formula where parameters a,b,c,d and e are determined through substitution calibration.

$$W = a \cdot \frac{mW^5}{5} + b \cdot \frac{mW^4}{4} + c \cdot \frac{mW^3}{3} + d \cdot \frac{mW^2}{2} + e \cdot mW$$

Density of water is calculated from formula

$$\rho_w = \frac{1000}{(1 - 4,6699 \cdot 10^{-10} \cdot p_{atm}) + 8 \cdot 10^{-5} \cdot (\theta - 4 + 2,1318913 \cdot 10^{-3} \cdot p_{atm})^2 - 6 \cdot 10^{-6} \cdot (\theta - 4 + 2,1318913 \cdot 10^{-3} \cdot p_{atm})^3}$$

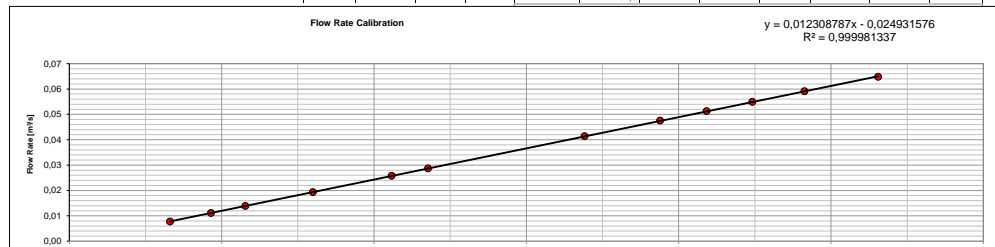
Density of air is calculated from formula

$$\rho_a = \frac{(p_{atm} \cdot 3,4837 \cdot 10^3)}{(273,15 + \theta)}$$

Discharge is found from formula

$$Q = \frac{W_2 - W_1}{\rho_w \cdot t \cdot (1 - \frac{\rho_a}{\rho_w})}$$

Time	Manual Observation before Weight	Manual Observation Weight	Manual Observation Q	Manual Observation Q	Time	Ambient pressure P_{atm}	Water temp T_w	Air temp T_a	Calculated value before Weight	Calculated value after Weight	Differential weight	Density of water	Density of air	Differential volume	Calculated Flow Rate Q	Estimate Q	Deviation
	[kg]	[kg]	[m³/s]	[m³/s]		[kPa]	[°C]	[°C]	[kg]	[kg]	[kg]	[kg/m³]	[kg/m³]	[m³]	[m³/s]	[m³/s]	[%]
11.01.2012	21238.4	22172.7		2,661159	120.103	99.380	13.57	18.1	21222.7	22155.8	833.1	999.3631	1.1895	0.934817	0.0077834	0.00803	3.12547
11.01.2012	22172.7	23506.2		2,930580	120.103	99.380	13.65	18.1	22155.8	23487.6	1331.7	999.3631	1.1895	1.33417	0.0111085	0.01137	2.31726
11.01.2012	23506.2	25170.4		3,155332	120.102	99.380	13.73	18.1	23487.6	25149.5	1661.9	999.3521	1.1895	1.66496	0.0138629	0.01416	2.07245
11.01.2012	25170.4	27494.5		3,598328	120.103	99.380	13.81	18.1	25149.5	27470.2	2320.7	999.3411	1.1895	2.32501	0.0193585	0.01964	1.45362
11.01.2012	27494.5	30596.0		4,116114	120.103	99.380	13.89	18.1	27470.2	30556.9	3086.7	999.3299	1.1895	3.09243	0.0257462	0.02606	1.19023
11.01.2012	30596.0	34032.3		4,354587	120.103	99.380	13.97	18.1	30556.9	33997.3	3440.5	999.2845	1.1895	3.44705	0.0287008	0.02901	1.07432
11.01.2012	34032.3	39000.2		5,382559	120.103	99.380	14.05	18.1	33997.3	38956.0	4958.6	999.3074	1.1895	4.96800	0.0413645	0.04175	0.91596
11.01.2012	39000.2	44706.7		5,877990	120.103	99.380	14.13	18.1	38956.0	44650.5	5694.5	999.3187	1.1895	5.70517	0.0475024	0.04788	0.79744
11.01.2012	44706.7	50885.0		6,183233	120.103	99.380	14.21	18.1	44650.5	50797.1	6146.6	999.2960	1.1895	6.15824	0.0512746	0.05167	0.78658
11.01.2012	50885.0	57469.0		6,483198	120.103	99.380	14.29	18.1	50797.1	57380.2	6583.1	999.2730	1.1895	6.59578	0.0549177	0.05538	0.83736
11.01.2012	57469.0	64577.3		6,826085	120.103	99.380	14.37	18.1	57380.2	64467.1	7086.9	999.2614	1.1895	7.10056	0.0591206	0.05963	0.85270
11.01.2012	64577.3	72370.3		7,309225	120.103	99.380	14.45	18.1	64467.1	72234.8	7767.7	999.2614	1.1895	7.78275	0.0649006	0.06561	1.23989



Appendix F

Parts and Materials

Following are the order lists for the material, instruments and parts.

SMITH

E.A. Smith AS
7493 Trondheim

ORDREBEKREFTELSE

Ordrenr **0013082339**

Vårt momsreg nr NO816051142

Kunde

NTNU - ENERGI OG PROSESSTEKNIKK
KOLBJØRN HEJESVEI 1D
7491 TRONDHEIM

Kundenr

NTNUKL001

Godsmottaker

NTNU - ENERGI OG PROSESSTEKNIKK
VANNKRAFTLAB.- 73593858
ALFRED GETZ VEI 4
7491 TRONDHEIM

Deres referanse

BÅRD BRANDÅSTRØ

Ordredt

280911

Leveringsmåte

SMITH-BIL

Lev betingelse

DDP(Leveringsadr.)

Deres ordrenr

N11141169

Dato

290911

Valuta

NOK

Side:

1(1)

Vår referanse

ANNY EGGEN

Betal beting

30 dager etter leveringsdato

Selger

ANNY EGGEN

Lin	Artikkelnr	Beskrivelse	Antall		Salgspris	Beløp
Lev dato					Rabatt	
5	05242520	152,0x 79,4 mm (15085) - 3-6 m	0,52 M	54,964 KG	20,95	1.151,50
061011		EMNERØR S355 J2G3				
10	05242520KA	KAPP	1,00 STK	1,00 STK	122,00	122,00
061011		1 X 520 MM				
	TILRIG	tilrigging				110,00
15	05360159	16 mm tilskjærte plater NVE36	153,60 KG	153,60 KG	12,20	1.874,00
061011		STÅLPLATER				
		1 STK 480 X 2500 MM				
20	06239505	91,0 mm	1,30 M	66,43 KG	46,80	3.108,92
061011		RUSTFRITT SEIGHERDET AKSELSTÅL S165M/W.1.4418,SKALLDREID K12				
	LEG	LEGERINGSTILLEGG				873,55
25	06239505KA	KAPP	1,00 STK	1,00 STK	0,00	0,00
061011		1 X 1300 MM				
30	910S-0217697	. 232,70 X 148,4 MM - 1X470 MM	93,10 KG	93,10 KG	53,65	4.994,82
201011		EMNERØR OVAKO 280				
Avgifter						983,55
MVA-grunn						12.234,79
MVA						3.058,71
Ordretotal						15.293,50
Avrundning						0,50
Total						15.294,00

Med vennlig hilsen

E.A. Smith AS

ANNY EGGEN

Våre salgsbetingelser for stål og metaller, og byggevarer er oppdatert på www.smith.no (produktområder)

E.A. Smith AS

Avd. Smith Stål Nord TrondheimPostboks 9410 Sluppen

7493 TRONDHEIM

Tlf: 72592400

Fax: 72592301

<http://www.smith.no>

HBM Norge AS

p.b. 254, 1411 Kolbotn

Tel: +47 48300700

Fax: +47 66810000



Ordrebekreftelse

HBM Norge AS, p.b. 254, 1411 Kolbotn

NTNU- Institutt for energi- og
prosessteknikk
Kolbjørn Hejes v 1B
7491 TRONDHEIM

Salgsordrenr./ Dato

3800002207 / 12.12.2011

Kundenr.: 3010755

Tilbudsnr./Dato

9999224802 /08.12.2011

Salgsingeniør:

Bjarne Hauge

Bestillingsnr.: Bård Brandåstrø

Dato: 08.12.2011 / Telefon: 73 59 38 60

Bestiller:

Avdeling / Ordrebehandler

HBM Norge Rydland Laila

Tel. 047 - 48300700

Fax. 047 / 66810000

Email: Laila.Rydland@hbm.com

Leveringsadresse

NTNU- Institutt for energi- og
prosessteknikk
Kolbjørn Hejes v 1B
7491 TRONDHEIM

Incoterms:

CIF TRONDHEIM

Levering med:

TNT

Transportør:

TNT

Dietzenbach

Fraktkostnader:

Merking:

				Valuta: NOK
Pos.	Materiale	Antall	Pris	Total
0010	1-Z6FD1/5KG-1 Load cell Z6FD1/5KG I hht EC-bestemmelse 1207/2001, ingen preferanse berettigelse. Leveringsdato fra lager (Tyskland): Day 14.12.2011	1 PCS	NOK 2.580,00	2.580,00
Totalt antall denne pos.			NOK	2.580,00
Utgående mva.		25,000 %	NOK 2.580,00	645,00
Totalt			NOK	3.225,00

Betalingsbetingelser: Netto per 30 dager

Lieferbedingung:

Hvis ikke annet er avtalt, vil Deres ordre bli håndtert i hht våre generelle leveringsbetingelser.

Hochschule Luzern
Technik & Architektur
Herr Briggeler
Technikumstrasse 21
6048 Horw

RECHNUNG 444128

Kriens, 31.03.2008

Seite 1

Lieferschein 472449 vom 25.03.2008

Bestell-Datum/Art	Ihre Referenz	Bestell-Nummer	Kommission
25.03.2008/e-mail	Herr Briggeler Marc	HSLU T&A	

Transportart: abgeholt

u/Referenz: Urs Boppart

Artikel	Menge	Preis EUR	Preis CHF		Betrag CHF
6016-2RS1	2.00	79.75	122.85	NT	245.70 ✓
Rillenkugellager SKF					
KRV22-PP-A	1.00	46.15	71.04	NT	71.05 ✓
Kurvenrolle INA					
KRVE22-PP-A	1.00	60.55	93.28	NT	93.30 ✓
Kurvenrolle INA					
KRV40-PP-A	4.00	47.05	72.48	NT	289.90 ✓
Kurvenrolle INA					
KRVE40-PP-A	4.00	56.70	87.32	NT	349.30 ✓
Kurvenrolle INA					
KMK 15	1.00	73.45	113.12	NT	113.10 ✓
Wellenmutter SKF					
KMK 11	1.00	46.35	71.38	NT	71.40 ✓
Wellenmutter SKF					
ORS 6 mm NBR	2.00	3.75	5.78	NT	11.55 ✓
Rundgummischnur 70° Shore					
SE J 125x4	2.00	337.55 /%	519.82 /%	NT	10.40 ✓
Sicherungsring DIN 472					
SPASH 114x124x0.5 K3	1.00	592.50 /%	912.45 /%	NT	9.10 ✓
Ausgleichscheibe					
Verpackung 0.00	Porto 0.00	Auftragswert in EUR 821.30		Auftragswert in CHF 1'264.80	

Total-Warenwert	Verpackung	Porto	%	MWSt	Rechnungstotal in CHF	1'360.90 ✓
1'264.80	0.00	0.00	7.6	96.10	MWST-Nr. 155'863	

Wir danken für Ihren Auftrag.

Zahlung 30 Tage netto.

Hochschule Luzern – T&A		Buchungskreis: 1011	
Visum I:	Visum II:	Vis. Triage TS:	Vis. Triage D&S:
16.4.08	16.4.10		
Fibu	Kst/Ktr	Betrag	
61210	1120309	1360.90	
Total Rechnung		1360.90	

WÄRLZLAGER · ANTRIEBSTECIINIK · DICHTUNGEN

MONTALPINA AG · KREUZSTRASSE 51 · POSTFACH · CH-6000 Luzern

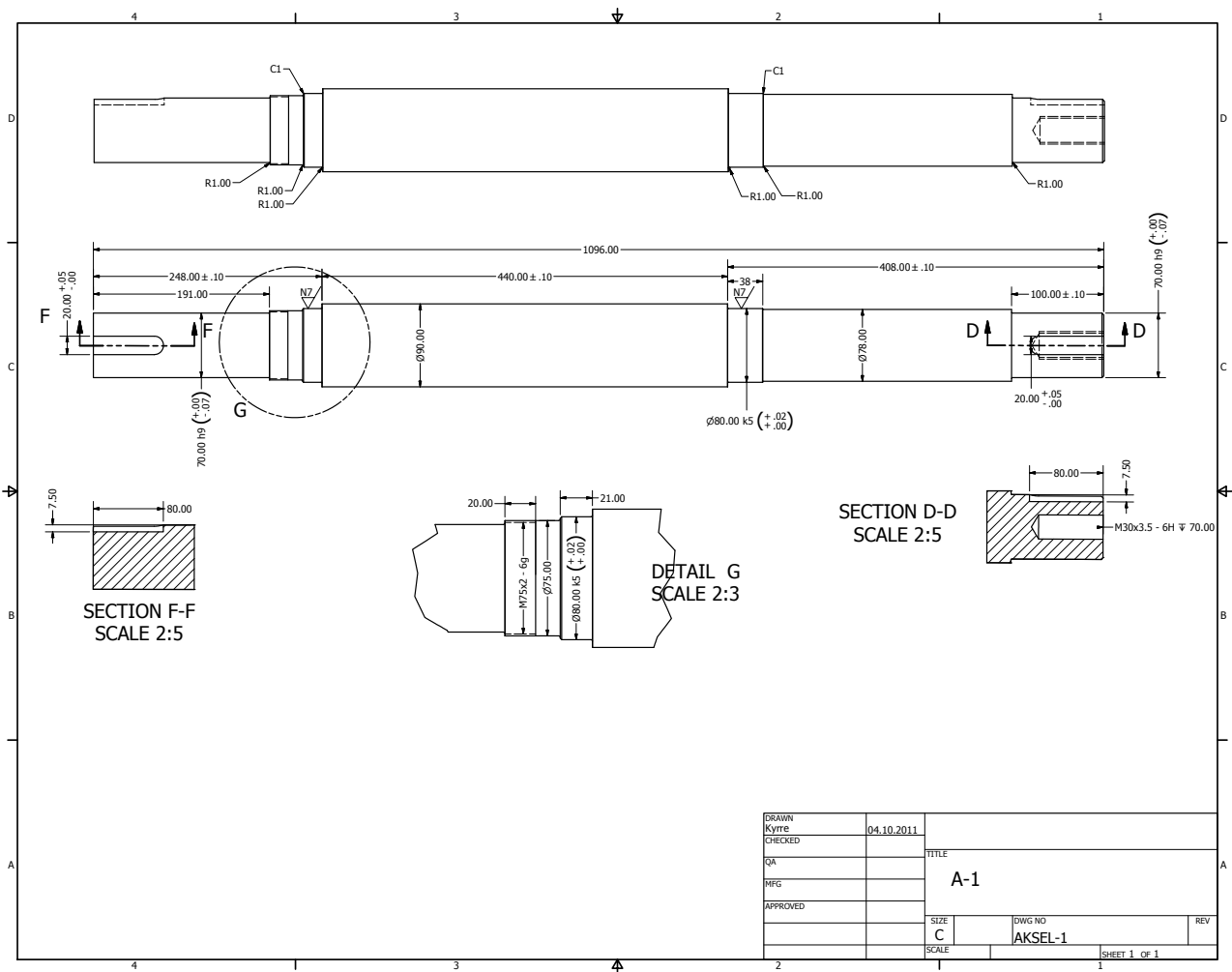
Fon +41 (0)41 348 0 348 · Fax +41 (0)41 348 0 349 · info@montalpina.com

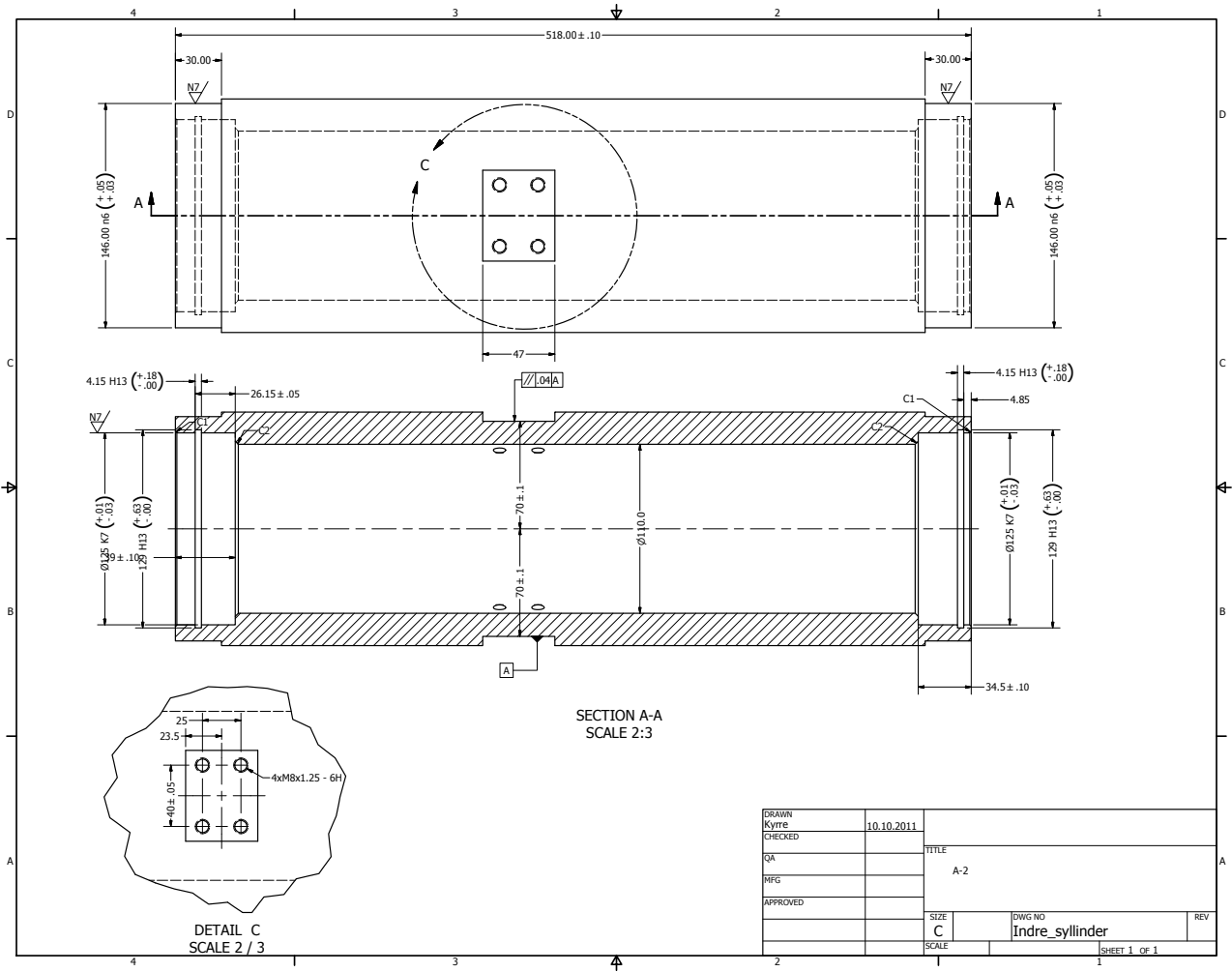


Appendix G

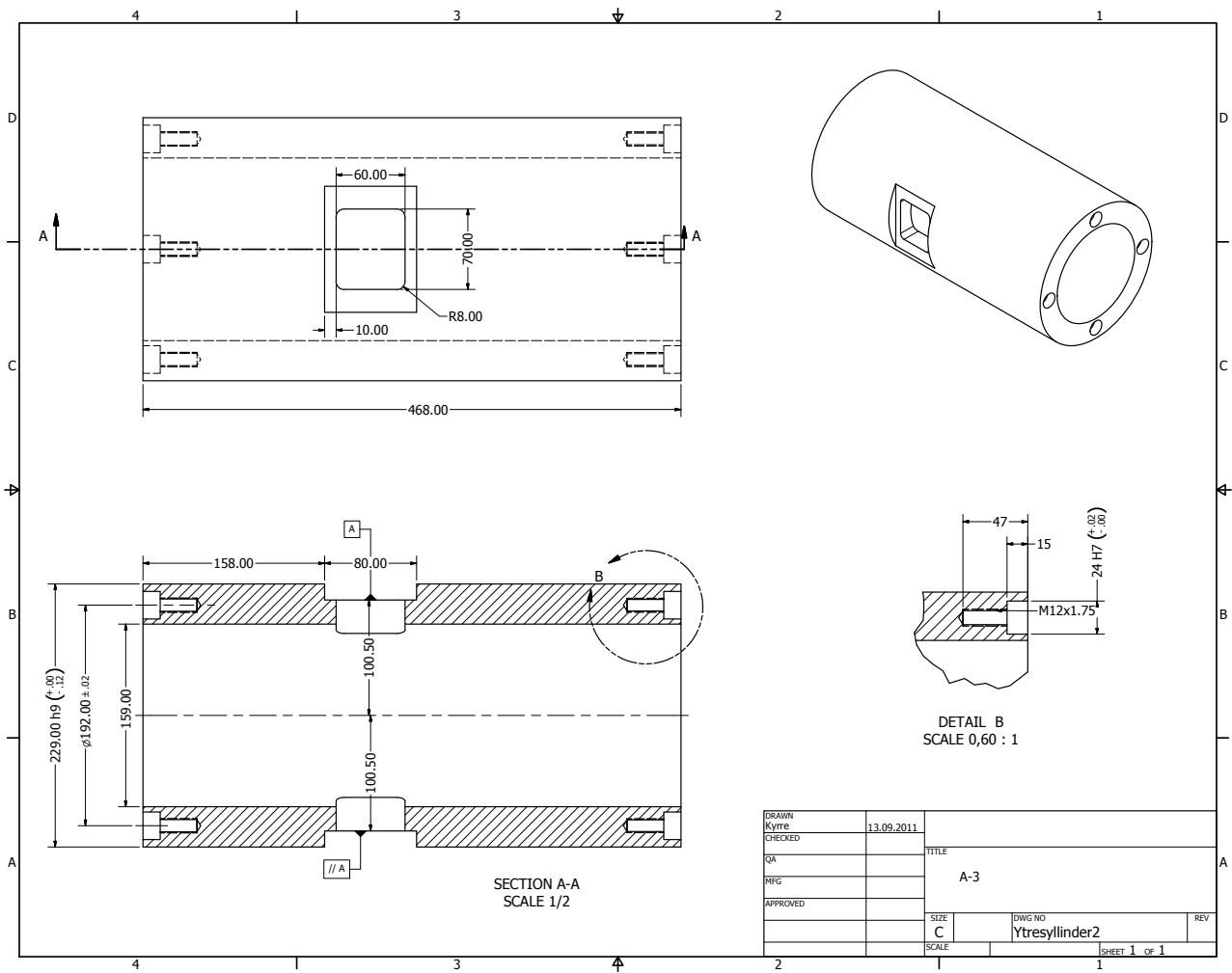
Machine Drawings

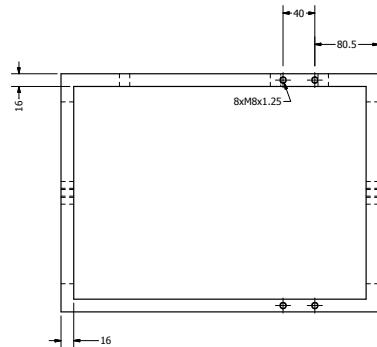
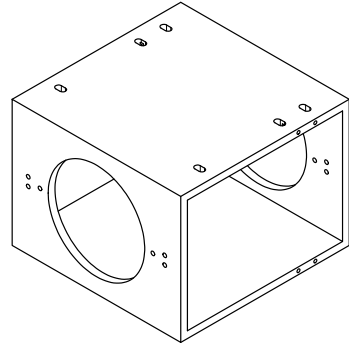
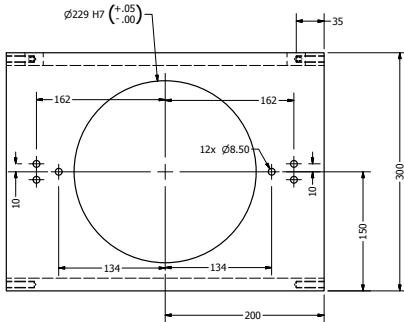
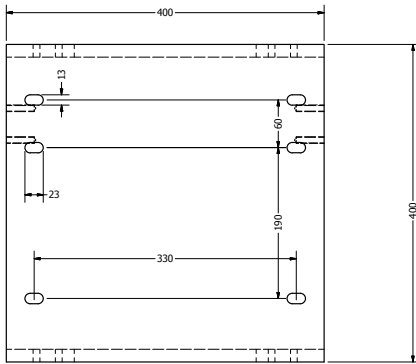
In this appendix are presented the Machine drawing that were created for the production of the bearing block. The first 11 were made by the auther , while the last 9 drawings were made at Hochschule Luzern.





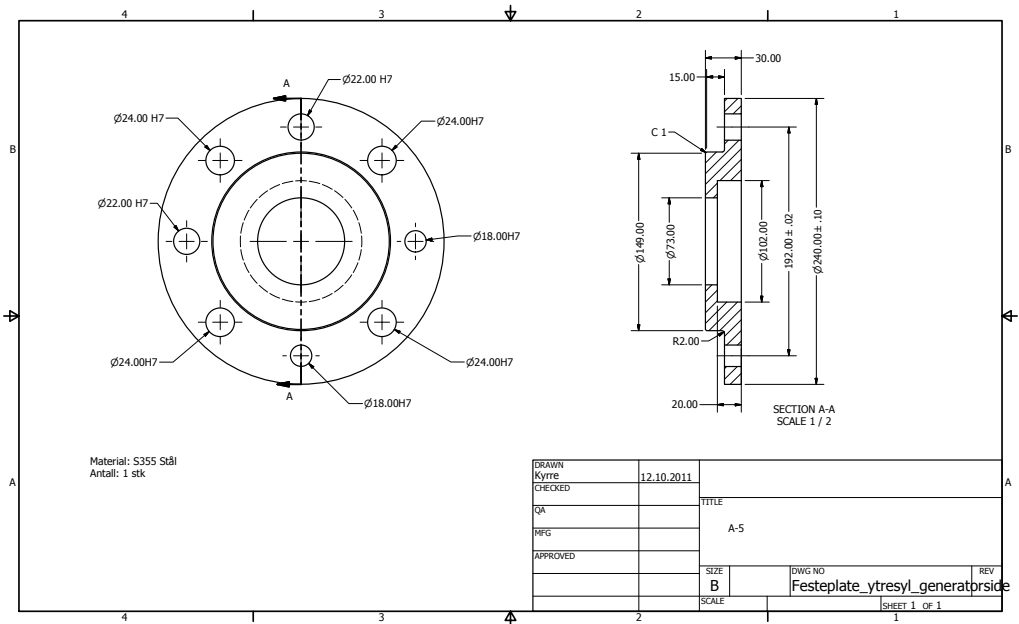
DRAWN	Kyrie	10.10.2011		
CHECKED			TITLE	
QA			A-2	
MFG				
APPROVED				
			SIZE	DWG NO
			C	Indre_syllinder
			SCALE	REV

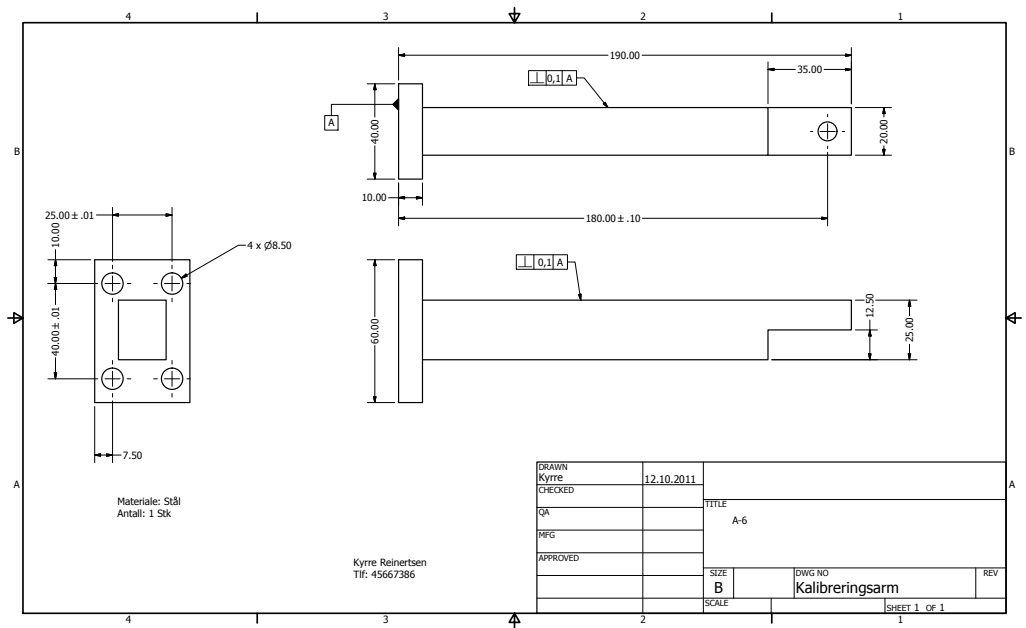


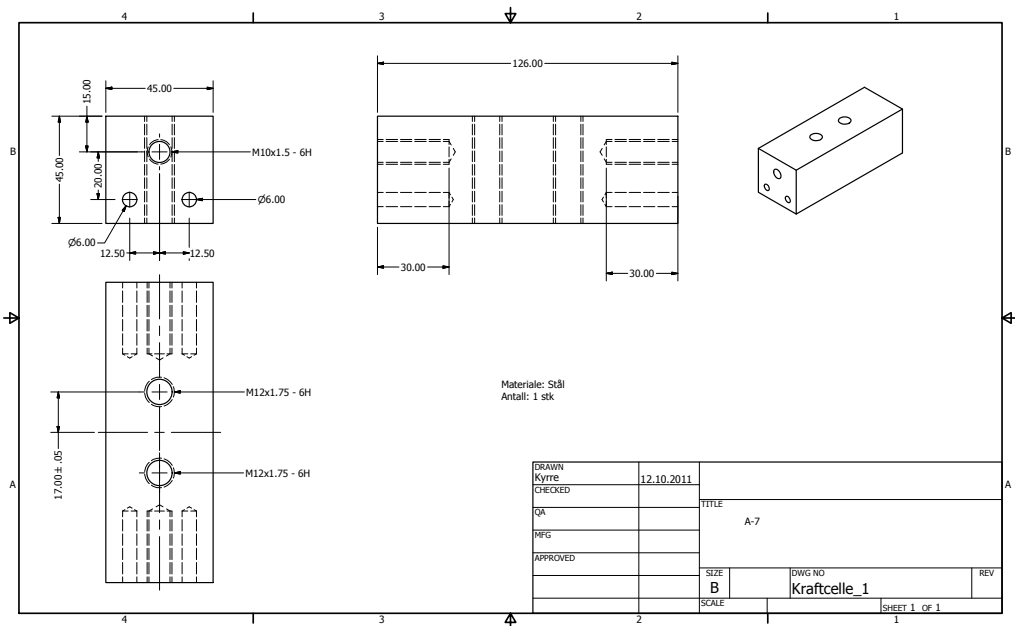


DRAWN	Kyrie	10.10.2011	TITLE	
CHECKED				
QA			A-4	
MFG				
APPROVED			SCALE	
			SIZE	DWG NO
			C	Boks
			SCALE	REV

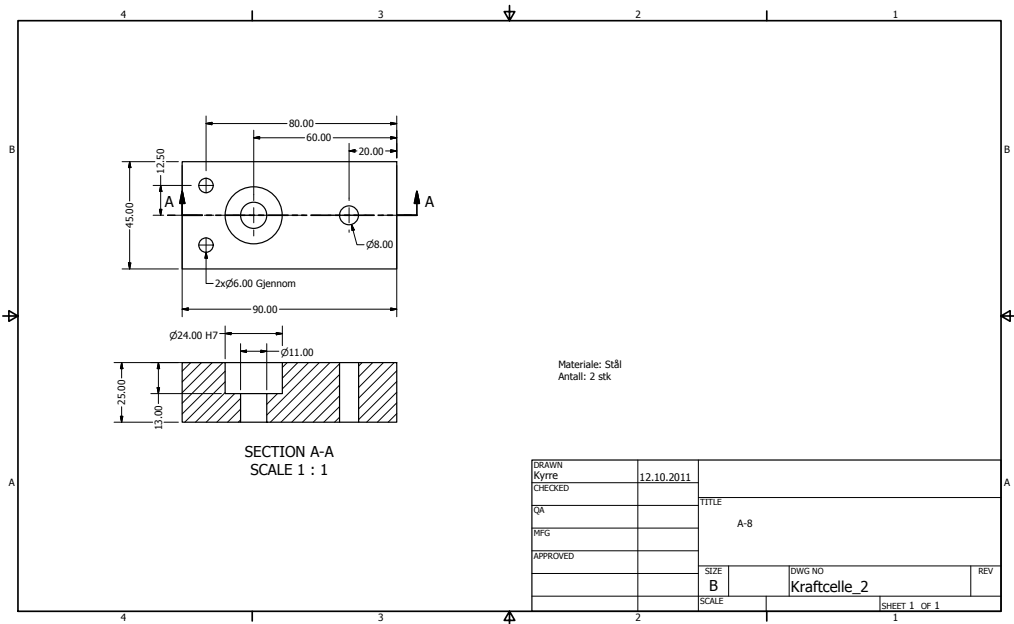
SHEET 1 OF 1

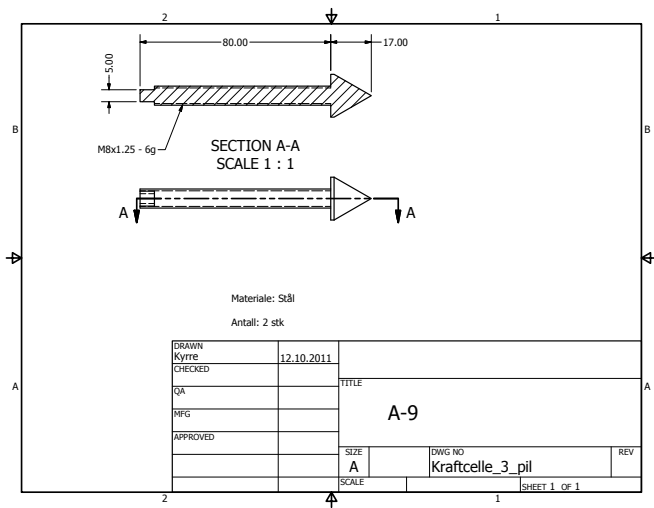


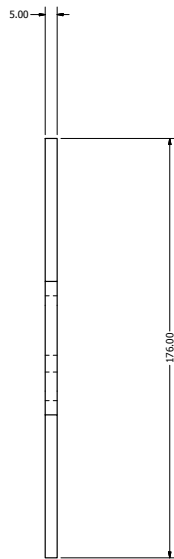
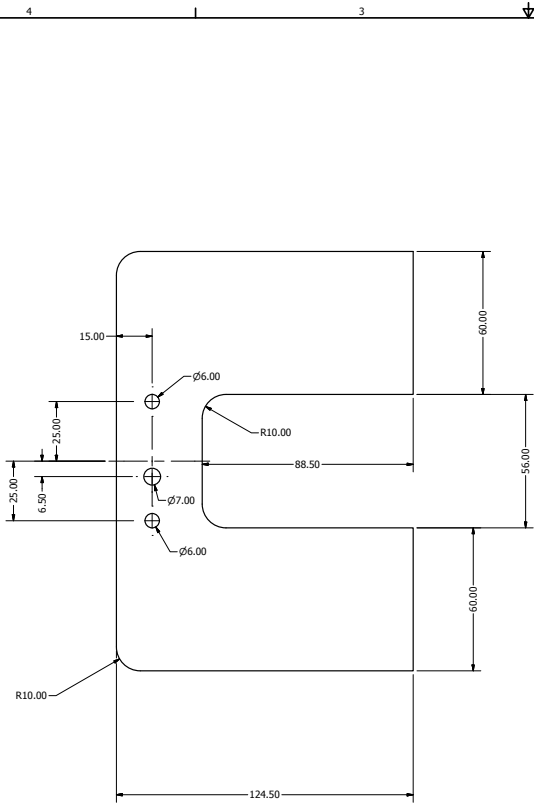




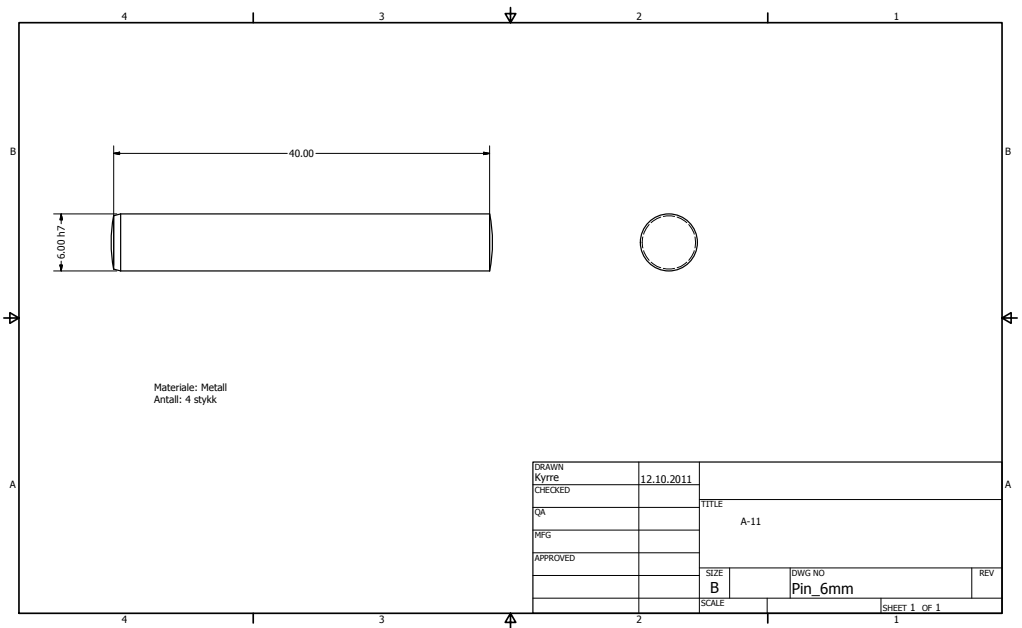
DRAWN	12.10.2011	TITLE	
Kyrtte			
CHECKED		A-7	
QA			
MFG		SIZE	
APPROVED			
		B	DWG NO
		Kraftcelle_1	REV
		SCALE	SHEET 1 OF 1

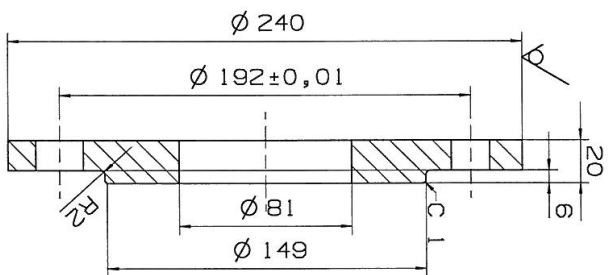







DRAWN	Kyrie	25.09.2011			
CHECKED			TITLE		
QA			A-10		
MFG					
APPROVED					
			SIZE	DWG NO	REV
			C	Stotteplate	
			SCALE	SHEET 1 OF 1	





The diagrams show the construction of a triangle with a vertical line segment. The first diagram shows a triangle with a vertical line segment inside it. The second diagram shows a triangle with a vertical line segment inside it, and a point on the line segment. The third diagram shows a triangle with a vertical line segment inside it, and a point on the line segment.

Anderungen / Modifications	 Ersatz fuer / Replacement for Ersetzt durch / Replaced by
Lagerung Peltonpruefstand	Messstab / Scale 12 x x
Flansch Loslagerseite	Gezahnelt / Prepared / M Bruegeleix Gebohrt / Drilled x x Gelesen / Approved x x

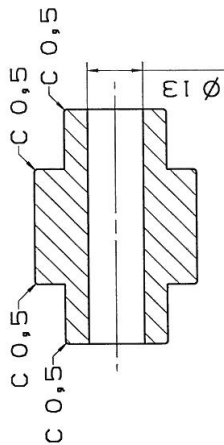
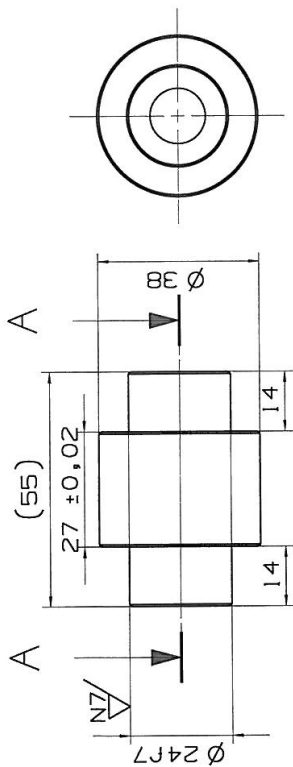
Lagerung Peltonpfeilstand

Flansch Loslagerseite

Lucerne University of Applied Sciences and Arts

HOCHSCHULE
LUZERN

Nr. 5



Schnitt A - A

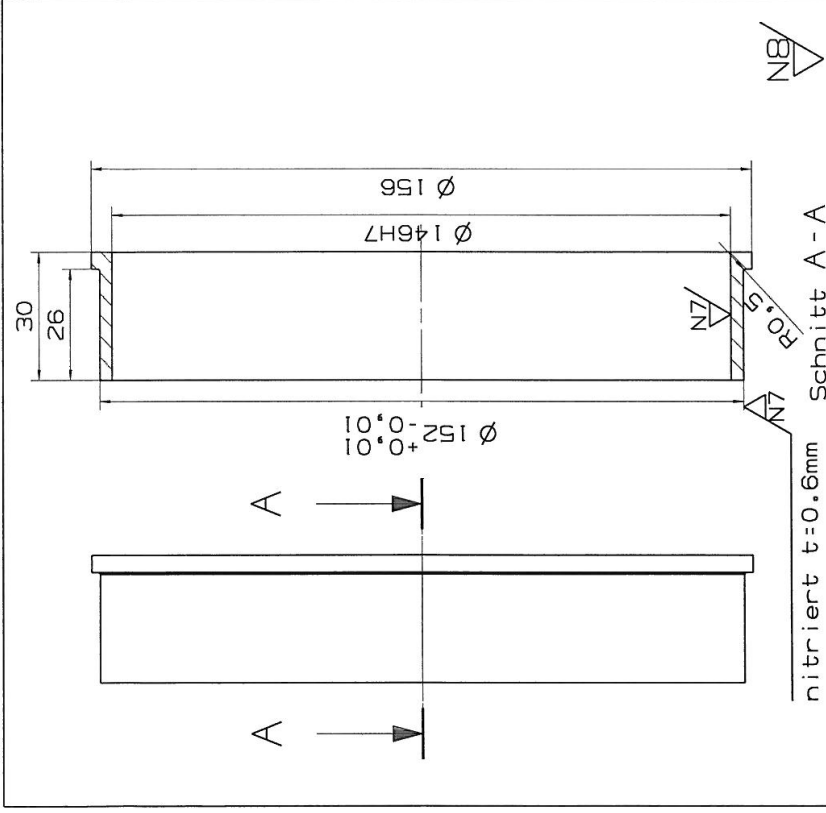
Anzahl: 8 Stueck

Material: S235



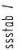
Kanten gebrochen 0.2x45Grad

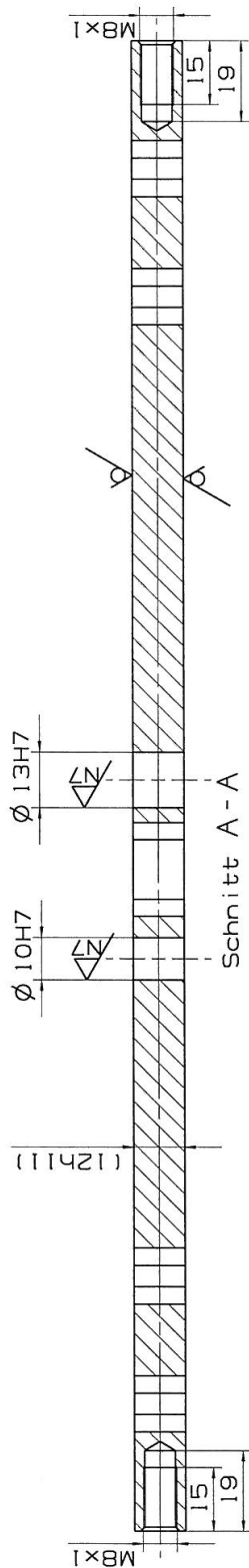
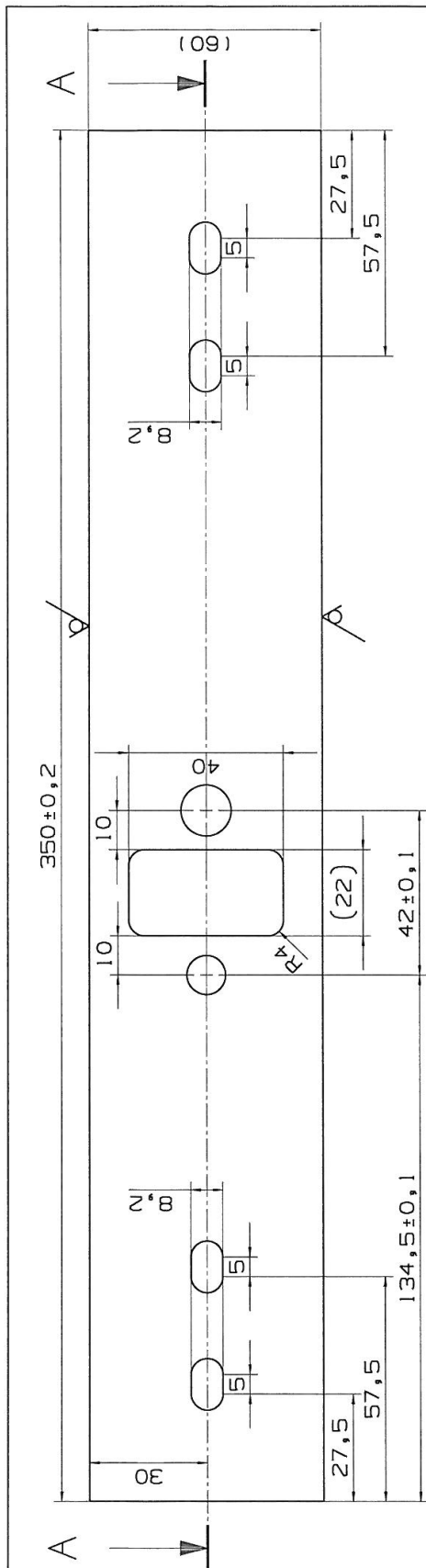
NB/ (N7/)

Änderungen / Modifications	G/A/D	Ersatz fuer / Replacement for Ersetzt durch / Replaced by			
		Gezeichnet / Prepared	Geprüft / Checked	M.Briggelenx	
Lagerung Peltonpruefstand	Massstab / Scale	1:1	x	x	
Distanzwelle	x	x	x	x	
	x	Gesehen / Approved	x	x	
Modell-Zeichung Nr. / Model-, DWG-Nummer / Sheet					1/1
HSLU HOCHSCHULE LUZERN Lucerne University of Applied Sciences and Arts Technik & Architektur Engineering & Architecture					Nr. 6



Kanten gebrochen 0.2x45Grad Material: 34CrNiMo6

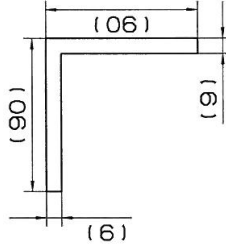
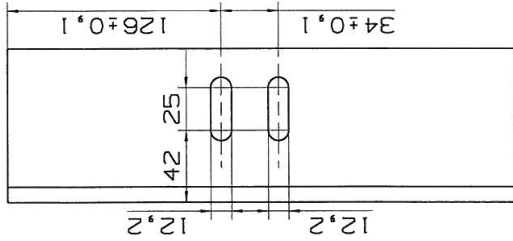
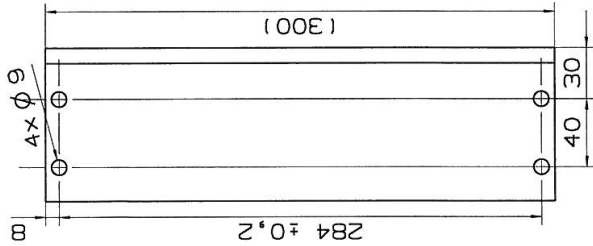
Änderungen / Modifications		Ersatz fuer / Replacement for			
		Ersetzt durch / Replaced by			
		Gezeichnet / Prepared			
		Geprüft / Checked			
Lagerung Peltonpruefstand		Gesehen / Approved			
		Modell-Zug Nr. / Model- DWG No			
		Blatt / Sheet			
		1/1			
Ring		Nr. 11			




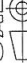
Kanten gebrochen 0.2 x 45Grad
Material S235

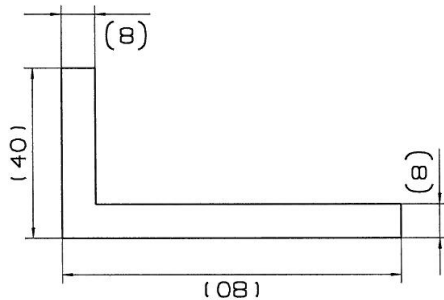
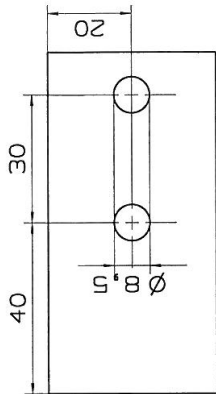
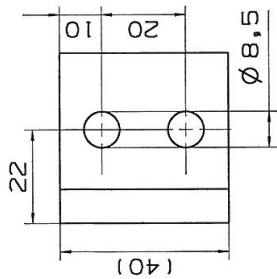
$$\left(\frac{\Delta_{\text{Zn}}}{\Delta_{\text{Zn}}} \right)$$

	Aenderungen / Modifications	GAD 	Ersatz fuer / Replacement for Ersetzt durch / Replaced by
Lagerung Peltonpruefstand	Massstab / Scale	1:1	Gesetzel / Prepared M-Binggeleix Geprueft / Checked
Axialplatte	x	x	x
HSLU	Lucerne University of Applied Sciences and Arts HOCHSCHULE LUZERN Technik & Architektur Engineering & Architecture	Nr. 12	Gesehen / Approved Modell-/Zeichn.-Nr. / Model- / DWG No. Blatt / Sheet 1 / 1





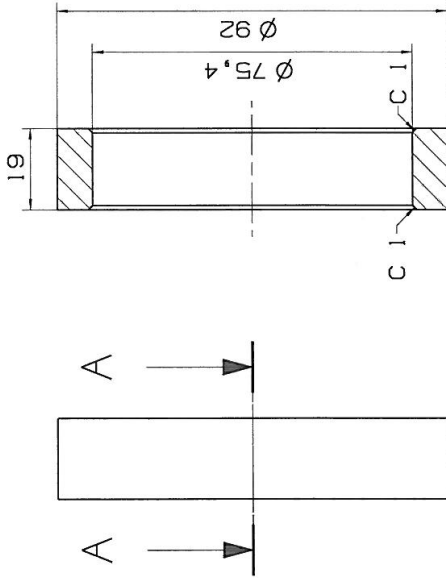
Kanten gebrochen 0.2.. 45Grad
Material: S235JR

Änderungen / Modifications		 		Ersatz fuer / Replacement for Ersetzt durch / Replaced by			
Lagerung Peltonpruefstand L-Profil_90x90x9		Massstab / Scale 1:25		Gezeichnet / Prepared		M.Braggelerich	
				Geprüft / Checked		x	
				Gesehen / Approved		x	
				Modell-Zeichn. Nr. / Model-, DWG No./Blatt / Sheet		1/1	
HSLU		Lucerne University of Applied Sciences and Arts		Nr. 13			
HOCHSCHULE LUZERN							
Technik&Architektur Engineering&Architecture							



Kanten gebrochen 0.2x45Grad
Material: S235JR+C

Änderungen / Modifications		 		Ersatz fuer / Replacement for Ersetzt durch / Replaced by	
Lagerung Peltonpruefstand Winkel 80x40		Massstab / Scale		Gezeichnet / Prepared	M. Briggelen
		1:1		Geprüft / Checked	x
		x			x
		x		Gesehen / Approved	x
HSLU Lucerne University of Applied Sciences and Arts HOCHSCHULE LUZERN Technik & Architektur Engineering & Architecture		Nr. 14		Modell-Zübing Nr. / Model-, DWG No. Blatt / Sheet 1/1	

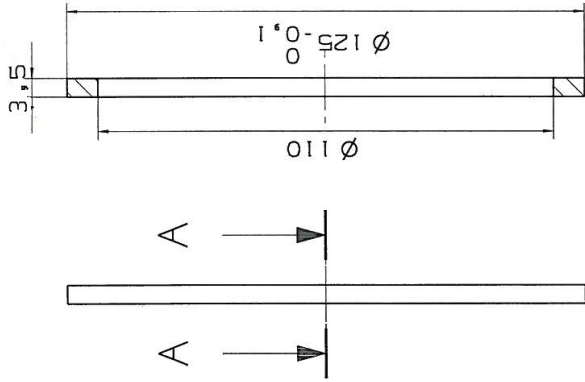


Schnitt A - A

Material: E355
Kanten gebrochen 0.2x45Grad

NB

Änderungen / Modifications Peltonpruefstand Lagerung Distanzring Festlager	GAID 	Ersatz fuer / Replacement for Ersetzt durch / Replaced by	
	Massstab / Scale 1:1 x x	Gezeichnet / Prepared Geprueft / Checked Gegeben / Approved	M.Briggelen x x x
	HSLU Lucerne University of Applied Sciences and Arts HOCHSCHULE LUZERN Technik & Architektur Engineering & Architecture	Modell-Zeichn. Nr. / Model., DWG No. Blatt / Sheet Nr. 18 1/1	





Schnitt A - A

NB/

radfren

Material: ~~E355~~

Kanten gebrochen 0.2x45Grad

Änderungen / Modifications				Ersatz fuer / Replacement for	
				Ersetzt durch / Replaced by	
Lagerung Peltonpruefstand		Massstab / Scale		Gezeichnet / Prepared	
		1:1		x	
Ring Abstand Wellenfeder		x		x	
		x		x	
				Gezeichnet / Approved	
				x	
				Modell-Zeichung Nr. / Model- DWG No. Blatt / Sheet	
				1/1	
				Nr 17	

G.1 Matlab Source Code

The following functions were created by Lorentz Fjellanger Barstad with the **MATLAB R2011b** distribution and are not tested with earlier versions of MATLAB.

G.1.1 Import Raw Data

```
%----- IMPORT PELTON RAW DATA -----  
%  
% This function import rawdata from .txt files of the form:  
  
%  
% | A | B | C | D | E |  
%  
% | a_1 | b_1 | c_1 | . | . |  
% | a_2 | b_2 | . | . | . |  
% | . | . | . | . | . |  
% | a_n | b_n | c_n | . | . |  
%  
% | A | B | C | D | E |  
%  
% | a_1 | b_1 | c_1 | . | . |  
% | . | . | . | . | . |  
% | a_n | b_n | c_n | . | . |  
%  
%  
% and return a matrix  
  
function [rawdata] = rawdata_import()  
  
    %Open file import dialog  
    [files,path] = uigetfile('*.txt','Import file(s) - (.txt) only','MultiSelect'  
  
    %Find number of files selected  
    if ischar(files) == 1  
        fileNum = 1;  
    else  
        fileNum = length(files);  
    end  
    %Loop through source files  
  
    for j = 1:fileNum
```

```

if fileNum == 1
    file = files;
else
    file = char(files(j));
end

filepath = [path, '', file];
file = dir(filepath);
fid = fopen(filepath);

pos = 1; %Byte number to start import
i = 2;
while pos < file.bytes

    [rawdata(i,j),pos] = textscan(fid, '%f %f %f %f %f %f ', 'HeaderLines
    'CollectOutput', 1);
    i = i+1;
end

rawdata{1,j} = file; %Set file info as column header
fclose(fid);

end
end

```

G.1.2 Calculate Mean Data

```

%———— CALCULATE MEAN DATA FROM RAW DATA (meandata_create.m) ————
%
%   Creates a new matrix 'meandata' from a source MxN:
%
%           1       .       .       .       N
%           ———— ———— ———— ———— ————
%   1 |   A   |   B   |   C   |   D   |   E   |
%   . |————|————|————|————|————|
%   |  a_1  |  b_1  |  c_1  |   .   |   .   |
%   . |  a_2  |  b_2  |   .   |   .   |   .   |
%   |   .   |   .   |   .   |   .   |   .   |
%   . |   .   |   .   |   .   |   .   |   .   |
%   |   .   |   .   |   .   |   .   |   .   |
%   M |  a_M  |  b_M  |       |   .   |   .   |
%   |————|————|————|————|————|
%
%   Where A-E indicates different nozzles (headers), and (a,b,c,...)_m is
%   measurements at

```

```

% different constant rotational speeds.
%
% OUTPUT      meandata      Nx1 struct table
%             meandata_spl  Nx1 struct table
%             nan_map       (M-1)xN table of '0' and '1' where '1' indicates
%                               that the source contains NaN values

% source      rawdata matrix (from rawdata_import.m)

function [meandata meandata_spl nan_map] = meandata_create(source)

%-----

D = 0.4786;           %Diameter of runner [m]
g = 9.82146514;      %Gravity in the NTNU laboratory
p_error = 0.207;      %Pressure transducer correction [m]
t = 1.960;           %Degrees of freedom (random uncertainty)

n11_a = 36;          %Reduced rot. speed (n_11) start
n11_b = 44;          %n_11 end
n11_step = 0.5;       %n_11 increment

%-----

s = size(source);
nan_map = zeros(s(1),s(2));

%Create 'meandata'

for j = 1:s(2)

    for i = 1:s(1)-1

        if isempty(source{i+1,j})

            p_temp(i,1) = NaN;
            q_temp(i,1) = NaN;
            T_temp(i,1) = NaN;
            M_temp(i,1) = NaN;
            Mlm_temp(i,1) = NaN;
            Mtot_temp(i,1) = NaN;
            n_temp(i,1) = NaN;
            q11_temp(i,1) = NaN;
            qed_temp(i,1) = NaN;
            n11_temp(i,1) = NaN;
            ned_temp(i,1) = NaN;

```

```

Ph_temp(i,1) = NaN;
Pm_temp(i,1) = NaN;
rho_temp(i,1) = NaN;
etah_temp(i,1) = NaN;
head_temp(i,1) = NaN;
Eh_temp(i,1) = NaN;
P_lm(i,1)=NaN;
nan_map(i,j) = 1;

else

p = source{i+1,j}(:,1);
q = source{i+1,j}(:,2);
T = source{i+1,j}(:,3);      %temperature
M = source{i+1,j}(:,4);      %torque
Mlm = source{i+1,j}(:,5);    %torque friction
n = source{i+1,j}(:,6);

%Mean values of raw data
p_temp(i,1) = mean(p);
q_temp(i,1) = mean(q);
T_temp(i,1) = mean(T);
M_temp(i,1) = mean(M);
Mlm_temp(i,1) = mean(Mlm);
Mtot_temp(i,1) = mean(M) + mean(Mlm); %total torque
n_temp(i,1) = mean(n);

%Calculate error and standard deviation of raw data
std_p = std(p);
std_q = std(q);
std_T = std(T);
std_M = std(M);
std_Mlm = std(Mlm);
std_n = std(n);

err_p = (t*std_p)/sqrt(length(p));
err_q = (t*std_q)/sqrt(length(q));
err_T = (t*std_T)/sqrt(length(T));
err_M = (t*std_M)/sqrt(length(M));
err_Mlm = (t*std_Mlm)/sqrt(length(Mlm));
err_n = (t*std_n)/sqrt(length(n)/1000);

p_temp(i,2) = err_p;
q_temp(i,2) = err_q;
T_temp(i,2) = err_T;
M_temp(i,2) = err_M;
Mlm_temp(i,2) = err_Mlm;
Mtot_temp(i,2) = sqrt(err_M^2 + err_Mlm^2);

```

```

n_temp(i,2) = err_n;

p_temp(i,3) = err_p/p_temp(i,1)*100;
q_temp(i,3) = err_q/q_temp(i,1)*100;
T_temp(i,3) = err_T/T_temp(i,1)*100;
M_temp(i,3) = err_M/M_temp(i,1)*100;
Mlm_temp(i,3) = err_Mlm/Mlm_temp(i,1)*100;
Mtot_temp(i,3) = Mtot_temp(i,2)/Mtot_temp(i,1)*100;
n_temp(i,3) = err_n/n_temp(i,1)*100;

% etah_temp(i,2) = sqrt(p_temp(i,3)^2 + q_temp(i,3)^2 + ...
%      T_temp(i,3)^2 + M_temp(i,3)^2 + n_temp(i,3)^2);

etah_temp(i,2) = sqrt(p_temp(i,3)^2 + q_temp(i,3)^2 + ...
      T_temp(i,3)^2 + Mtot_temp(i,3)^2 + n_temp(i,3)^2);

%Calc density (rhow), E, H, omega, q11_temp, Ph, Pm, eta, head_t
Pstat = p_temp(i,1);
rhow = 1000/ ( (1 - (4.6699e-10)*Pstat*1000) + ...
      (8e-6)*(T_temp(i,1) - 4 + (2.1318913e-7)*Pstat*1000)^2 - ...
      (6e-8)*(T_temp(i,1) - 4 + (2.1318913e-7)*Pstat*1000)^3 );

E = ((Pstat*1000)/rhow) + g*p_error + 0.5*(q_temp(i,1)...
      /(0.25*pi*0.1^2))^2;
H = E/g;
omega = ((2*pi)/60)*n_temp(i,1);
q11 = q_temp(i,1)/((D^2)*sqrt(H));
n11 = (n_temp(i,1)*D)/sqrt(H);
Ph = rhow*q_temp(i,1)*E;
Pm = Mtot_temp(i,1)*omega;
Plm=Mlm_temp(i,1)*omega;

q11_temp(i,1) = q11;
qed_temp(i,1) = q11/sqrt(g);
n11_temp(i,1) = n11;
ned_temp(i,1) = n11/sqrt(g);
Ph_temp(i,1) = Ph;
Pm_temp(i,1) = Pm;
Plm_temp(i,1) = Plm;
rho_temp(i,1) = rhow;
etah_temp(i,1) = Pm/Ph;
etam_temp(i,1)=(Pm-Plm)/Pm;
eta_temp(i,1)=(Pm-Plm)/Ph;
head_temp(i,1) = H;
Eh_temp(i,1) = E;

```

end

```

end

%Insert calculated data into new table 'meandata'

noz = source{1,j};
b = length(noz)-7;
%From raw
meandata{j,1}.nozzle = noz; %noz(1:b)
meandata{j,1}.p = p_temp;
meandata{j,1}.q = q_temp;
meandata{j,1}.temp = T_temp;
meandata{j,1}.torque = M_temp;
meandata{j,1}.torque_lm = Mlm_temp;
meandata{j,1}.torque_tot = Mtot_temp;
meandata{j,1}.n = n_temp;
%Calculated
meandata{j,1}.q11 = q11_temp;
meandata{j,1}.qed = qed_temp;
meandata{j,1}.n11 = n11_temp;
meandata{j,1}.ned = ned_temp;
meandata{j,1}.power_h = Ph_temp;
meandata{j,1}.power_m = Pm_temp;
meandata{j,1}.power_lm=Plm_temp;
meandata{j,1}.density = rho_temp;
meandata{j,1}.etah = etah_temp;
meandata{j,1}.etam = etam_temp;
meandata{j,1}.eta = eta_temp;
meandata{j,1}.head = head_temp;
meandata{j,1}.energy = Eh_temp;

clear q11_temp qed_temp n11_temp ned_temp eta etahmek Ph_temp Plm_temp P
      etah_temp head_temp Eh_temp p_temp q_temp T_temp n_temp

end

% Create 'meandata_spl' where the etah is estimated by a spline and the
% volume flows are avaraged

meandata_spl = meandata;

s = size(meandata_spl);

ideal_ned = (n11_a:n11_step:n11_b)/sqrt(g);

for i = 1:s(1)

    old_eta = meandata{i,1}.etah(:,1);
    old_ned = meandata{i,1}.ned(:,1);
    ss = size(old_eta);

```

```

for ii = 1:ss(1)

    if nan_map(ii,i) == 1    %Datarange contains NaN values >> Must estim
                            %eta and q

        %Calculate average volume flows
        q_sum = 0; q11_sum = 0; qed_sum = 0; mc = 0;
        for m = 1:ss(1)

            if isnan(meandata{i,1}.q(m,1)) == 0

                q_sum = q_sum + meandata{i,1}.q(m,1);
                q11_sum = q11_sum + meandata{i,1}.q11(m,1);
                qed_sum = qed_sum + meandata{i,1}.qed(m,1);
                mc = mc + 1;
            end
        end

        meandata_spl{i,1}.q(ii,1) = q_sum/mc;
        meandata_spl{i,1}.q11(ii,1) = q11_sum/mc;
        meandata_spl{i,1}.qed(ii,1) = qed_sum/mc;

        %Estimate the missing datapoint
        aa = old_ned(1); bb = old_ned(end);

        ned_step = (bb - aa)/(length(old_ned)-1);

        ned_r = old_ned(1):ned_step:old_ned(end);

        new_eta = spline(old_ned,old_eta(:,1),ned_r);

        meandata_spl{i,1}.etah(ii,1) = new_eta(ii);

        %n_ED
        meandata_spl{i,1}.ned(ii,1) = ideal_ned(ii);

    end

end

end

```

G.1.3 Efficiency Curve Fit

```

%———— (meandata_spline.m) —————%

```



```

function [meandata_fitted] = meandata_fit(source,a)

    %source = meandata_spl;

    rows = length(source);

    g = 9.82146514;

    ned_ideal = (36:0.5:44)/sqrt(g);
    ned_len = a*length(ned_ideal);
    ned_step = (44-36)/(ned_len-1);
    ned_new = (36:ned_step:44)/sqrt(g);

    % Set up fitttype and options.
    ft = fitttype( 'smoothingspline' );
    opts = fitoptions( ft );
    opts.SmoothingParam = 0.975726050374513;

    meandata_fitted = source;

    for i = 1:rows

        qed(i) = mean(source{i,1}.qed);

        x_sp = source{i,1}.ned(:,1);
        y_sp = source{i,1}.etah(:,1);

        [xData, yData] = prepareCurveData(x_sp,y_sp);

        %[fitresult, gof]
        fitresult = fit(xData,yData,ft,opts);

        %val = coeffvalues(fitresult);
        %values(i,1) = val;

        for ii = 1:ned_len

            meandata_fitted{i,1}.etah(ii,1) = fitresult(ned_new(ii));
            meandata_fitted{i,1}.ned(ii,1) = ned_new(ii);

            eta(ii,i) = fitresult(ned_new(ii));

```

```

end

clear val
% % Plot fit with data.
% figure( 'Name', 'untitled fit 1' );
% h = plot( fitresult, xData, yData );
% legend( h, 'y_sp vs. x_sp', 'untitled fit 1', 'Location', 'NorthEast'
% % Label axes
% xlabel( 'x_sp' );
% ylabel( 'y_sp' );
% grid on

end

%
%
% fit ned = konst
%
% qed_len = a*length(qed);
%
% qed_step = (qed(end)-qed(1))/(qed_len - 1);
%
% qed_new = qed(1):qed_step:qed(end);
%
% for i = 1:170
%
%     x_sp = qed; %Qed
%     y_sp = eta(i,:);
%
%     [xData, yData] = prepareCurveData(x_sp,y_sp);
%
%     %[fitresult, gof]
%     fit_q = fit(xData,yData,ft,opts);
%
%     %meandata_fitted{i,1}.etah(ii,1) = fitresult(ned_new(ii));
%     %meandata_fitted{i,1}.ned(ii,1) = ned_new(ii);
%
%     for j = 1:qed_len
%
%         %eta(i,j) = fit_q(qed_new(j));
%
%     end
%
%     clear fit_q xData yData
%
% end
%
```

```

%figure
%contour(n_ed_spl,Q_ed,eta_spl',50);

end

```

G.1.4 Plot Hill Chart

```

%———— PLOT EFFICIENCY HILL DIAGRAM (meandata_hillplot.m) —————

function [qed ned eta map] = meandata_hillplot(source)

    rows1 = length(source);
    rows2 = length(source{1,1}.etah);

    g = 9.82146514;
    qed = zeros(1,rows1);
    ned = (36:0.5:44)/sqrt(g);
    eta = zeros(rows2,rows1);
    %map = eta;
    %map_ned = eta;

    k = 1;

    for i = 1:rows1

        qed(i) = mean(source{i,1}.qed);

        for ii = 1:rows2
            eta(ii,i) = source{i,1}.etah(ii,1);

            %map(k,1) = source{i,1}.qed(ii,1);
            %map(k,2) = source{i,1}.ned(ii,1);
            %map(k,3) = ned(ii);

            k = k + 1;
        end
    end

```

```

        %err_plot(j,i) = source{i,1}.eta_h(j,2);
    end

end

%Create a figure of (ned,qed,eta) = (x,y,z)
figure

set(gcf,'paperOrientation','landscape','paperUnits','normalized','paperType','a4');
[c] = contour(ned,qed,'eta',[0.85:0.004:0.89 0.89:0.001:0.8939 0.8939:0.0001:0.894]);
[c] = contour(source{1,1}.ned(:,1),qed,'eta',[0.85:0.005:0.88 0.88:0.003:0.885]);
clabel(c);
xlabel('n_{ED}');
ylabel('Q_{ED}');
%set(gca,'fontsize',14);
set(gca,'xtickmode','manual','xtick',11:0.5:14.5);
grid on

end

```

G.1.5 Uncertainty due to the Regression Process

This script was made by Lars Fjærvold to calculate the uncertainty and proved to work also for this project.

```

%% Leser inn data fra Veietanken og de loggede voltverdiene
clear all
clc
temp=rawdatas_import();
yi=xlsread('Q.xls');
lengde=length(temp);
t=1.960;
yavg=mean2(yi);
%% Finner summen av alle voltverdiene ved alle målepunktene og hvor mange
% punkter det i hver måleserie

for i = 1:lengde
    nan_locations = find(isnan(temp{2,i}));
    temp{2,i}(nan_locations) = 0;
    m_rows(i) = size(temp{2,i},1);
    n_cols(i) = size(temp{2,i},2);
    tot_x(i) = sum(sum(temp{2,i}));
end

```

```

        temp2(i)=mean2(temp{2,i});
        x_values(i) = temp(2,i);
end
totalx=sum(tot_x);
xavg=mean2(temp2);

%% Regner ut Sxx Syy og Sxy og b. Kjører tre for-løkker for å hente ut hver
% eneste enkeltverdi fra matrisene

for i = 1:lengde
    x_temp = x_values(i);
    for j = 1:m_rows(i)
        for k = 1:n_cols(i)
            y = yi(i);
            y_temp2(j,k) = (y-yavg)^2;
            x = x_temp{1,1};
            x_temp2(j,k) = (x(j,k)-xavg)^2;
            xy_temp2(j,k) = (x(j,k)-xavg)*(y-yavg);
        end
    end
    y_temp3(i)=sum(sum(y_temp2));
    x_temp3(i)=sum(sum(x_temp2));
    xytemp3(i)=sum(sum(xy_temp2));
    maxtemp(i)=max(max(x));
    mintemp(i)=min(min(x));
    i
end

Sxx = sum(x_temp3)
Syy = sum(y_temp3)
Sxy = sum(xytemp3)

b=Sxy/Sxx

%% Setter inn kalibreringsligningen som er funnet ved å benytte excel:

%% Regner ut varians og standardavvik og finner confidensintervallet
% plotter så usikkerheten.

s2 = (Syy-b*Sxy)/(totalx-2)

s=sqrt(s2)

A=max(maxtemp);
B=min(mintemp);

for x0=1:8

```

```

Y(x0) = (0.012415793*x0-0.024820801)*1000
%   Y(x0) = 81.49352283*x0-162.87533823;
con_interval(x0)=t*s*sqrt((1/totalx)+(((x0)-xavg)^2)/Sxx);
yeah(x0) = Y(x0)+con_interval(x0)*10000;
yeah2(x0) = Y(x0)-con_interval(x0)*10000;
end

plot(Y)
xlabel('Volt [V]')
ylabel('Volume flow [l/s]')
title('Calibration curve with 95% confidence interval scaled by 1000')
grid on
hold on
plot(yeah, 'color', 'red')
hold on
plot(yeah2, 'color', 'red')
hold on

```